Effects and risk assessment of halogenated bisphenol A derivatives on human follicle stimulating hormone receptor: An interdisciplinary study

Valentine Suteau, Lorena Zuzic, Ditlev Høj Hansen, Lisbeth R Kjølbye, Paul Sibilia, Louis Gourdin, Claire Briet, Mickaël Thomas, Éric Bourdeaud, Hélène Tricoire-Leignel, et al.

Journal of Hazardous Materials 479 (2024) 135619

Contents lists available at ScienceDirect

Journal of Hazardous Materials

journal homepage: www.elsevier.com/locate/jhazmat

Effects and risk assessment of halogenated bisphenol A derivatives on human follicle stimulating hormone receptor: An interdisciplinary study

Valentine Suteau [a,d,1], Lorena Zuzic [b,1], Ditlev Høj Hansen [b], Lisbeth R. Kjølbye [b], Paul Sibilia [a,d], Louis Gourdin [a,e], Claire Briet [a,d,e], Mickaël Thomas [c], Eric Bourdeaud [c], Hélène Tricoire-Leignel [a], Birgit Schiøtt [b,f], Pascal Carato [c], Patrice Rodien [a,d,e], Mathilde Munier [a,d,e,*]

[a] Angers University, MITOVASC, CarMe Team, CNRS UMR 6015, INSERM U1083, Angers, France
[b] Department of Chemistry, Aarhus University, 8000 Aarhus C, Denmark
[c] Poitiers University, Ecology & Biology of Interactions Laboratory, CNRS UMR 7285, INSERM CIC1402, IHES Research Group, Poitiers, France
[d] Department of Endocrinology, Diabetology and Nutrition, University Hospital Angers, Angers, France
[e] Centre de Référence des Maladies Rares de la Thyroïde et des Récepteurs Hormonaux, University Hospital Angers, Angers, France
[f] Interdisciplinary Nanoscience Center (iNANO), Aarhus University, 8000 Aarhus C, Denmark

HIGHLIGHTS

- Effects of chlorinated and brominated BPA derivatives (Cl_xBPA or Br_xBPA) on the FSHR activity.
- BPA and Cl_xBPA and B_xBPA are negative allosteric modulator on FSHR signalling.
- BPA exhibits stable binding in the inactive FSHR conformation.
- Study evaluated the risks of Cl_xBPA derivatives using a new approach methodology.

GRAPHICAL ABSTRACT

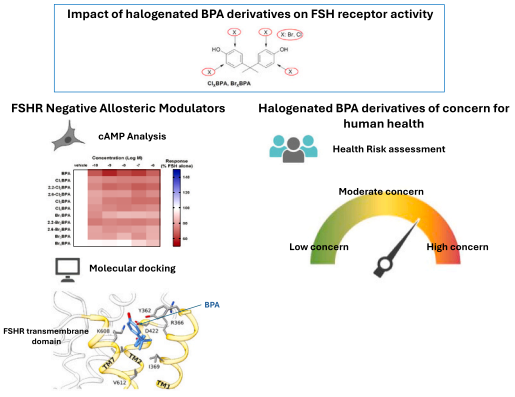

ARTICLE INFO

Keywords:
Endocrine disruptors - Bisphenol A - FSH/FSH receptor signaling - Molecular docking and dynamics simulations - Health risk

ABSTRACT

Halogenated bisphenol A (BPA) derivatives are produced during disinfection treatment of drinking water or are synthesized as flame retardants (TCBPA or TBBPA). BPA is considered as an endocrine disruptor especially on human follicle-stimulating hormone receptor (FSHR). Using a global experimental approach, we assessed the effect of halogenated BPA derivatives on FSHR activity and estimated the risk of halogenated BPA derivatives to

Abbreviations: BPA, Bisphenol A; mono-, ClxBPA, bi-, tri- and tetrachlorinated BPA derivatives; BrxBPA, mono-, bi-, tri- and tetrabrominated BPA derivatives; FSHR, follicle-stimulating hormone receptor; LHCGR, luteinizing hormone/choriogonadotropin receptor; RMSD, Root mean square deviation; HQ, hazard quotient; LOEC, lowest effective concentration; UF, Uncertainty Factor; NOEC, no-observed-effect concentration; TM, transmembrane helix; ECL, extracellular loop.

* Correspondence to: Laboratoire MITOVASC UMR CNRS 6015 - INSERM U1083, Bâtiment IRIS2, 3 rue Roger Amsler, 49100 Angers, France.
E-mail address: mathilde.munier@univ-angers.fr (M. Munier).

[1] Co-first authors

https://doi.org/10.1016/j.jhazmat.2024.135619
Received 6 May 2024; Received in revised form 20 August 2024; Accepted 21 August 2024
Available online 29 August 2024

the reproductive health of exposed populations. For the first time, we show that FSHR binds halogenated BPA derivatives, at 10 nM, a concentration lower than those requires to modulate the activity of nuclear receptors and/or steroidogenesis enzymes. Indeed, bioluminescence assays show that FSHR response is lowered up to 42.36 % in the presence of BPA, up to 32.79 % by chlorinated BPA derivatives and up to 27.04 % by brominated BPA derivatives, at non-cytotoxic concentrations and without modification of basal receptor activity. Moreover, molecular docking, molecular dynamics simulations, and site-directed mutagenesis experiments demonstrate that the halogenated BPA derivatives bind the FSHR transmembrane domain reducing the signal transduction efficiency which lowers the cellular cAMP production and *in fine* disrupts the physiological effect of FSH. The potential reproductive health risk of exposed individuals was estimated by comparing urinary concentrations (through a collection of human biomonitoring data) with the lowest effective concentrations derived from in vitro cell assays. Our results suggest a potentially high concern for the risk of inhibition of the FSHR pathway. This global approach based on FSHR activity could enable the rapid characterization of the toxicity of halogenated BPA derivatives (or other compounds) and assess the associated risk of exposure to these halogenated BPA derivatives.

1. Introduction

Bisphenol A (BPA) is the most produced organic compound with over 6 million tons manufactured annually worldwide [1]. Its chemical structure consists of two phenol rings and two methyl groups connected by a methylene bridge [2] (Fig. 1). BPA is well known as an endocrine-disrupting chemical altering the reproductive function [3]. It is mainly used as a stabilizer or antioxidant in polycarbonate plastics or epoxy resins, from which it can migrate into water [4]. Microplastics also contribute to the accumulation of BPA in drinking water distribution systems [5].

In water, BPA can react with various substances such as hypochlorite ions, stemming from sodium hypochlorite which is added to tap water as a disinfectant in some places in the world [6]. This results in chlorine substitution in the phenolic aromatic rings leading to mono-, bi-, tri- and tetrachlorinated BPA derivatives (Cl_xBPA) [7] (Fig. 1). Similarly, bromine is produced by oxidation of bromide during the chlorination stage, or by complexation with bromide ions (Br^-) present in wastewater treatment plants [8,9], leading to mono-, bi-, tri- and tetrabrominated BPA derivatives (Br_xBPA) [10,11] (Fig. 1). Disinfection, the ultimate drinking water treatment process, plays an essential role in preventing the spread of diseases. Chlorine technologies, with Ultraviolet (UV) and ozone, are commonly used for this process because of their high oxidizing power and low economic cost. There are methods of disinfecting water that do not generate halogenated by-products (such as chlorine dioxide), but they are very expensive. To remove halogenated by-products from drinking water, different purification procedures are being developed, such as microporous organic networks [12], Cu/Fe bimetallic nanoparticles [13], or electrocatalytic processes [14]. Processes for decontaminating water from BPA, without producing halogenated by-products, e.g., by enzymatic degradation [15] or by using biological treatment [16] are currently being developed. Less costly approaches are necessary for controlling the generation of toxic by-products in wastewater containing halogen ions.

Halogenated BPA analogues, such as tetrabromobisphenol A (TBBPA or Br_4BPA) and tetrachlorobisphenol A (TCBPA or Cl_4BPA), mainly used as flame retardants [17], are partially dehalogenated in the environment under anaerobic conditions [18-21], or by pyrolysis [22] that results in complete dehalogenation into the BPA product. Br_4BPA and Cl_4BPA are persistent, lipophilic, and bioaccumulative, leading to biomagnification within the food chain.

In the environment, there are various sources of exposure to halogenated BPA derivatives, such as wastewater treatment plants and sewage sludge [23]. The main route of exposure to these emerging compounds is drinking water. Among halogenated BPA derivatives quantified in the drinking water of a French cohort of pregnant women, ClBPA had the highest detection rate (51%) and Cl_2BPA the highest concentration (maximum: 100 ng/L), while Br_3 and Br_4BPA were detected at very low levels (1%) and concentrations (<limit of quantification) [24]. Cl_xBPA have also been detected in food contact papers:

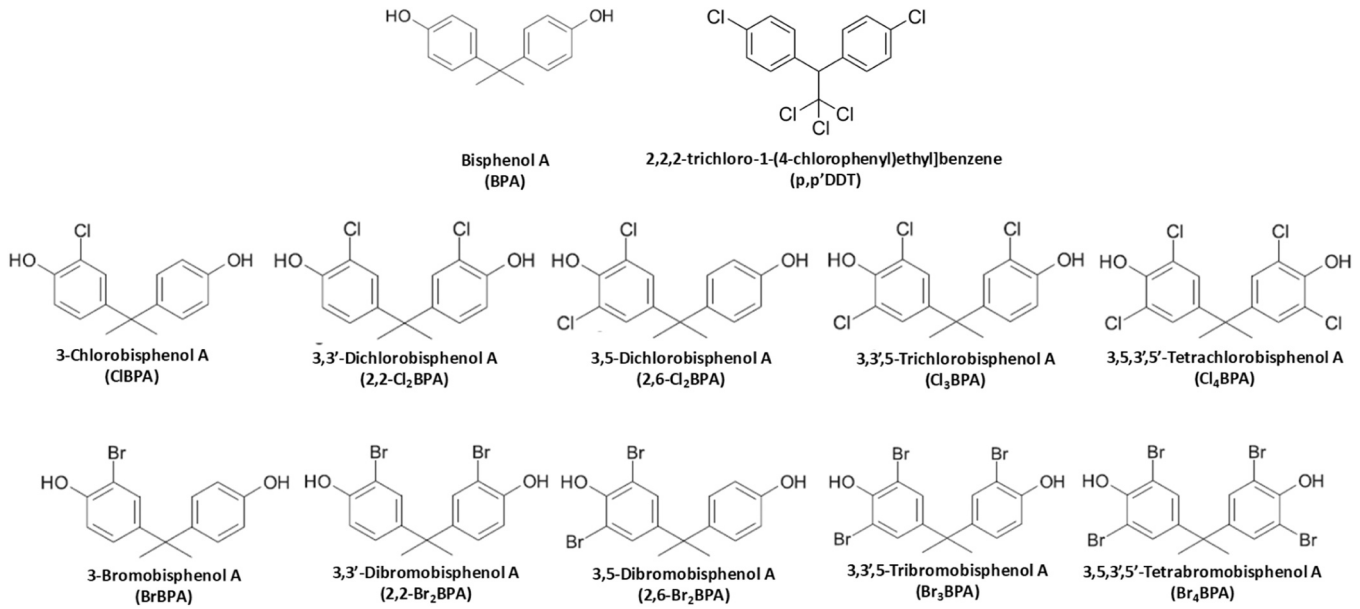

Fig. 1. Structure of investigated compounds. Modified from *Doumas* et al., *Chemosphere, 2018*.

ClBPA is the compound detected most frequently (41%) and in the highest concentration (0.016 ng/g) compared with other Cl_xBPA [25]. Cl_xBPA can migrate from food packaging to food. Halogenated BPA derivatives are also detected in human samples [23,26], demonstrating that humans are exposed to these compounds. Because these compounds are more lipophilic than BPA, their absorption and storage in organisms is more efficient [27]. Currently, there are no regulations regarding the tolerable threshold for halogenated BPA derivatives in drinking water in either Europe, the US or in Canada. Despite that, halogenated BPA derivatives could be considered as an emerging group of endocrine-disrupting chemicals that may contribute to adverse effects on human health, depending on the level of exposure of the population. However, the endocrine disruption potency of these compounds remains unknown.

Previously, we showed that non cytotoxic BPA concentrations reduce the response of the follicle-stimulating hormone receptor (FSHR) to FSH [28], a gonadotropin hormone involved in the regulation of gonadal function and fertility [29,30]. FSHR belongs to the G protein-coupled receptor (GPCR) or 7TM superfamily [31]. It consists of 7 transmembrane (TM) helices, 3 extracellular loops (ECL) and 3 intracellular loops (ICL). This receptor possesses a large extracellular domain that binds FSH. Hormone binding leads to a conformational change in the receptor, inducing an interaction between the TM helices of the FSHR and the Gs protein. Activation of the Gs protein leads to an activation of a signaling cascade resulting in an increased production of cyclic AMP (cAMP) in the cell. Currently, the effect of halogenated BPA derivatives on FSH receptor signaling is unknown. Determining the direct interaction mechanisms between BPA and halogenated BPA derivatives is crucial for understanding the mode of action of the chemicals.

To better understand the potential effect of halogenated BPA derivatives on FSHR activity, we studied the impact of 10 halogenated BPA derivatives on FSHR and compared with BPA. Real-time bioluminescence assays of FSHR activity make it possible to directly quantify the effect of halogenated BPA derivatives on receptor signaling and to determine their efficacy and potency. Molecular docking identified potential binding sites and the preferred orientation of the bound compounds. Molecular dynamics simulations were used to estimate the most stable conformation of the ligand-receptor complex, and to elaborate on the movements of the FSHR in the presence of the compounds. Site-directed mutagenesis was used to experimentally validate potential binding sites and to understand the binding mechanisms and the FSHR residues involved in this binding. This combined approach provides a comprehensive and detailed understanding of how halogenated BPA derivatives modulate FSHR activity (from theoretical predictions to experimental validation). Finally, the potential health risks of halogenated BPA derivatives were assessed by comparing the bioactive concentrations derived from the in vitro assay with the exposure levels established from biomonitoring data. The novelty of this study is its multi-dimensional approach, from the molecular interactions between chemical compounds and the receptor, to the assessment of the danger for exposed populations.

2. Materials and methods

2.1. Reagents

BPA was purchased from Sigma-Aldrich (# 239658) and halogenated BPA derivatives were synthetized as previously described [10]. All compounds were dissolved as stock solution at 1 M in dimethyl sulfoxide (DMSO, #P60–36720100, Pan Biotech) and stored at −20 °C in glass vials. Final DMSO concentration in each cell culture well was 0.1%. The human hFSH was purchased from Merck-Serono (Gonal-f), and stored at 4 °C. The low molecular weight agonist of FSHR 16a was kindly provided by J. Wrobel (Chemical and Screening Sciences, Wyeth research, Collegeville, PA) [32], and stored at room temperature. Forskolin was purchased from VWR (# CAYM11018).

2.2. Creation of the CHO-GLO and CHO-FSHR-GLO cell lines

To monitor the cAMP response of the FSHR in living cells, we generated clones of CHO-FSHR stably expressing a chimeric protein joining firefly luciferase (*Photinus pyralis*) to the cAMP-binding domain of protein kinase A, which upon cAMP binding emits light in the presence of substrate (D-luciferin) [33]. Two cell types, namely Chinese Hamster Ovary (CHO) cell line (RRID:CVCL_0214) native and CHO cell line stably transfected with the human FSHR (named CHO-FSHR) [28], were transfected with a plasmid encoding to an engineered cAMP sensitive luciferase (pGLO sensor™-22 F cAMP plasmid, GenBank® accession number is GU174434 - Promega) by the Lipofectamine LTX method (#10573013 – Fisher Scientific). The cells were seeded in 10-mm petri dishes 1 day before transfection. 2.5 µg of pGLO sensor™-22 F cAMP plasmid, containing the hygromycin B resistance gene, was transfected with 5 µL Lipofectamine LTX reagent. 24 h after transfection, selection was initiated with 400 µg/mL hygromycin B (# 30–240-CR, Corning). 12 hygromycin B-resistant clones for CHO-FSHR-GLO and 9 hygromycin B-resistant clones for CHO-GLO were isolated after 7 days and expanded using the same medium. Then, the 21 clones were selected based on their response to 10^{-5} M of forskolin (# CAYM11018, VWR) as a measure of expression of the reporter, and to 30 UI/mL FSH (for CHO-FSHR-GLO clones) in order to verify that the activity of the FSHR is maintained. All experiments were done using the clone #11. As expected, this cell line displayed the strongest luminescence response to forskolin and to FSH (Fig. S1). The cells were maintained in Dulbecco's modified Eagle's Medium (DMEM, #P04–03500, PAN Biotech) containing 10% heat-inactivated fetal calf serum (FCS, #S1810, Biowest), 2 mM glutamine (#BE17–605 F, Lonza), 100 U/mL penicillin, 100 µg/mL streptomycin (#17–602E, Lonza), 400 µg/mL geneticin (# 30–234-CR, Corning) and 400 µg/mL hygromycin B (# 30–240-CR, Corning), at 37 °C in a humidified incubator gassed with 5% CO_2. The cell lines were free of mycoplasma (Mycoplasma detection by PCR, Venro GeM OneStep, #11–8250, Minerva Biolabs).

2.3. GloSensor assay

Cells were seeded (100,000 cells/well) in white 96-well clear-bottom microplates (Greiner BioOne) with a medium containing DMEM, 10% heat-inactivated charcoal-stripped FCS (# 12676029, Life Technologies), 2 mM glutamine, 100 U/mL penicillin and 100 µg/mL streptomycin. The charcoal-stripped FCS ensured that the experiments were not influenced by steroid hormones. The following day, the cells media was replaced by 40 µL of DMEM with 6% v/v GloSensor cAMP reagent (# E1291 - Promega) and 10% heat-inactivated charcoal-stripped FCS and incubated for 2 h at room temperature. Firefly luciferase activity was measured at room temperature using FlexStation III multimode microplate reader (# FV05794, Molecular Devices) and real-time chemiluminescent signal was quantified for 1 h (2 min intervals and 1000 ms integration). The area under curve (AUC) for cAMP production was calculated for each condition. For data normalization, the AUC from hormone alone was set as 100%. For each analysis, at least three independent experiments were performed in triplicate.

2.4. MTT assay

Cell viability was determined using a 3-(four, 5-dimethylthiazol-2-yl)-two, 5-diphenyltetrazolium (MTT) (# M2128, Sigma-Aldrich) colorimetric assay. Cells were incubated with MTT solution (0.5 mg/mL) for 3 h at 37 °C, 5% CO_2. The absorbance of blue formazan crystals was measured at 570 nm using FlexStation® 3 Multimode Plate Reader. The results were expressed as a percentage of viability compared to the cells in absence of halogenated BPA derivatives (mean ± SEM of three independent experiments performed in triplicate).

2.5. Alanine-scanning mutagenesis

FSHR mutants were generated by GeneCust (Dudelange, Luxembourg), from the pSVL Plasmid (U138668) containing the human FSHR sequence (NM_000145.4) and transient transfected in CHO cell lines using Metafectene PRO (T040–1.0, Biontex) following the manufacturer's instructions. All the mutated plasmids were sequenced for control.

2.6. Docking and molecular dynamics simulations

Details about molecular docking and molecular dynamics simulations are provided in Supplementary Section S1. Briefly, using MODELLER 9.20 [34], the transmembrane domain of FSHR (from I1.29 to S7.69) was modelled in an inactive ($FSHR_{inact}$) and active ($FSHR_{act}$) conformation using homology modelling with luteinizing hormone/choriogonadotropin receptor (LHCGR) as a template (Fig. S2) [35]. The structures of 3-((5methyl)−2-(4-benzyloxyphenyl)−5-{[2-[3-ethoxy-4-methoxy-phenyl)-ethylcarbamoyl]-methyl}−4-oxo--thiazolidin-3-yl)-benzamide (16a), BPA, p,p′-DDT and their derivatives were built in Maestro 2020–1 in the Schrödinger 2020 suite. Induced fit dockings (IFDs) were built in Schrödinger Suite 2020 [36,37]. The molecular dynamics simulations were performed using GROMACS version 2019.4 simulation suite [38] and CHARMM36m force field [39]. The simulations were performed on eight different systems in a different combination of FSHR conformations and allosteric modulators BPA, p,p′-DDT, and 16a (Table S1). Root mean square deviation (RMSD) calculations were based on all heavy atoms in a ligand and were performed using MDAnalysis software package. Clustering of ligand conformations produced in molecular dynamic simulations was based on *gromos* algorithm [40] implemented in the Gromacs package.

2.7. Literature search on biomonitoring data

Full text articles in English were searched in PubMed (up to 8 April 2022). Studies were examined following searches "chlorinated derivatives of bisphenol A or chlorobisphenol A" or "brominated derivatives of bisphenol A or bromobisphenol A" and "serum or plasma or blood or urine" and "human" in the title and/or abstract were included. 77 articles were identified. The first selection was conducted on the title and abstract, and two independent reviewers based the second one on full-text analysis. The following exclusion criteria were used: "pathology", "in vitro or in vivo studies", "and non-halogenated derivatives of BPA"; "sample environment"; "non-human". 13 articles were included (Table 2 and S2).

2.8. Health risk assessment

The hazard quotient (HQ) model was used for preliminary human health risk assessment by comparing the measured urinary concentration of halogenated BPA derivatives with the lowest effective concentration (LOEC), which corresponds to the first tested concentration that induces a statistically significant effect compared to the control on the activity of the FSHR.

$$HQ = \frac{Measured\ urinary\ level(nM) \quad xUF}{LOEC(nM)}$$

Measured urinary level was estimated from biomonitoring data. Uncertainty Factor (UF, reflects the scientific uncertainty) = 1000 was used (10x individual human variability; 10x for LOEC to no-observed-effect concentration (NOEC) extrapolation; 10x for insufficient data and the use of urine concentrations instead of blood concentrations). HQ ≤ 1 indicated an absence of risk for the endpoint considered, whereas HQ ≥ 1 indicated that the exposure may be regarded as being of concern.

2.9. Statistical analyses

Data were analyzed in GraphPad Prism 8 (GraphPad Software Inc, La Jolla, CA). The difference between exposed and unexposed cells was evaluated using non-parametric Kruskal-Walli's test or one-way Dunn's multiple comparisons test. The comparisons between BPA and halogenated BPA derivatives were made using Welch's-test.

3. Results and discussion

3.1. Effects of halogenated BPA derivatives on FSH-dependent cAMP production

Guided by the previous study addressing the dose-response curve for FSH on hFSHR [28], we examined the effects of BPA and halogenated BPA derivatives on the response to two concentrations of FSH: 0.03 IU/mL and 3 IU/mL, corresponding to the EC_{50} and the C_{max}, respectively. Each compound was tested at five concentrations, including the ones reported in drinking water (i.e, from 10^{-11} to 10^{-8} M for BPA [10], from 10^{-12} to 10^{-10} M for Cl_xBPA [24,10,41] and from 10^{-14} to 10^{-10} M for Br_xBPA [24]), in human blood (i.e., from 10^{-9} to 10^{-7} M for BPA [42,43], from 10^{-12} to 10^{-10} M for Cl_xBPA [42,43], and from 10^{-10} to 10^{-8} M for Br_xBPA [44-47,43], or in human urine (i.e., from 10^{-10} to 10^{-8} M for BPA [48,27,49-51], from 10^{-11} to 10^{-10} M for Cl_xBPA [48,27,49], and from 10^{-10} to 10^{-9} M for Br_xBPA [47,50,51]. In CHO-FSHR-GLO cells, BPA reduced the EC_{50} or C_{max} FSH-induced cAMP accumulation up to 42.36 ± 4.41% (for 10^{-9} M BPA) or 29.82 ± 5.54% (for 10^{-6} M BPA), respectively, without effect on receptor basal activity (i.e., independent of FSH) (Fig. 2A, B, C). The 3-((5methyl)−2-(4-benzyloxy-phenyl)−5-{[2-[3-ethoxy-4-methoxyphenyl)-ethylcarbamoyl]-methyl}−4-oxo--thiazolidin-3-yl)-benzamide (16a) (a low molecular weight agonist of FSHR) can stimulate the FSHR with the same efficiency as FSH through binding to transmembrane domain [52]. 10^{-6} M BPA decreased by 14.78 ± 3.19% the low molecular weight agonist (16a)-induced maximal response (Fig. 3). None of the halogenated BPA derivatives had any impact on FSHR basal activity (Fig. 2D, G). In contrast, Cl_xBPA decreased cAMP production stimulated by both FSH concentrations. The 0.03 IU/mL FSH (EC_{50}) and 3 IU/mL FSH (C_{max}) induced responses were lowered up to 32.79 ± 4.62% (for 10^{-7} M 2,2-Cl_2BPA, Figs. 2E) and 27.95 ± 6.97% (for 10^{-9} M Cl_4BPA, Fig. 2F), respectively. 2,6-Cl_2BPA had no effect on C_{max} induced response. In the same way, Br_xBPA reduced FSH induced cAMP production at both FSH concentrations, except for Br_4BPA which had no effect. Indeed, 0.03 IU/mL FSH (EC_{50}) and 3 IU/mL FSH (C_{max}) induced responses are lowered up to 27.04 ± 5.68% (for 10^{-10} M 2,2-Br_2BPA, Figs. 2H) and up to 19.83 ± 4.90%, (for 10^{-6} M BrBPA, Fig. 2I), respectively. It is worth noting that no cytotoxicity was observed at active concentrations of BPA and halogenated BPA derivatives (Fig. 4). We have previously shown that BPA had no direct impact on adenylate cyclase (cAMP producing enzyme) nor on phosphodiesterases (cAMP degrading enzymes) [53]. These results suggest that the halogenated BPA derivatives act as negative allosteric modulators on FSHR signalling.

At 3 IU/mL FSH (C_{max}) induced cAMP response, there was no statistically significant difference between the inhibitory effects of BPA and those of halogenated derivatives (p-value > 0.05; Table 1). In opposite, BPA was the most effective negative allosteric modulator, causing a reduction up to 42.36 ± 4.41% in 0.03 IU/mL FSH (EC_{50}) induced cAMP production at a concentration of 10^{-9} M. However, the effects of 2,2-Cl_2BPA and 2,6-Cl_2BPA were statistically comparable to the effect induced by BPA (p-value > 0.05), but with concentrations 100-times higher than those used for BPA (10^{-7} M vs. 10^{-9} M). Other halogenated BPA derivatives induced a significant reduction in FSH response, but in a lesser extent than what was observed for BPA (Table 1). Moreover, the negative allosteric modulator activity of Cl_xBPA on FSHR was apparently stronger than of Br_xBPA. This disparity might be due to

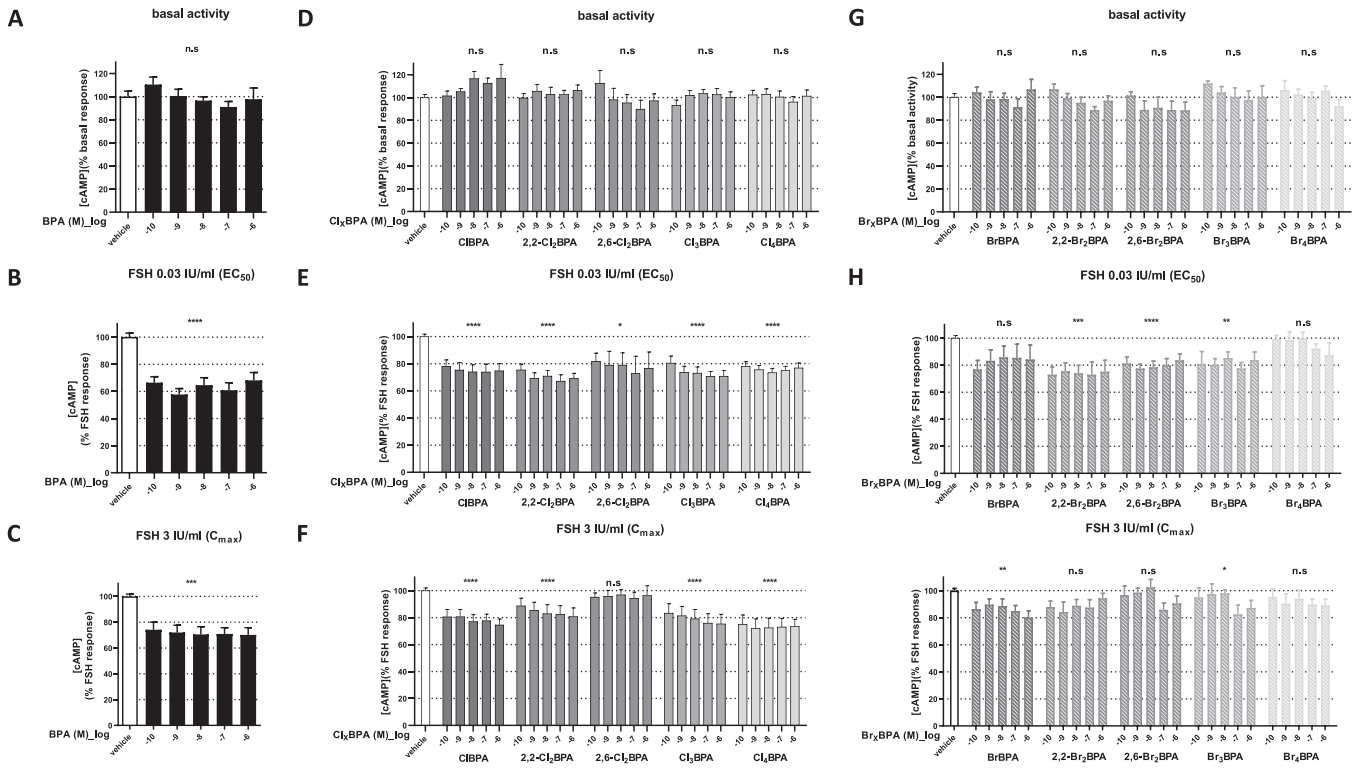

Fig. 2. Effect of halogenated-derivatives BPA on FSH-stimulated cAMP production. CHO-FSHR-GLO cells were incubated with five concentrations (from 10^{-10} to 10^{-6} M) of BPA, chlorinated BPA derivatives (Cl_xBPA) and brominated BPA derivatives (Br_xBPA), stimulated without (A, D,G) or with FSH 0.03 IU/mL (B, E, H) or 3 IU/mL (C, F, I). The cAMP concentration measured in the absence of Cl_xBPA (vehicle) was arbitrarily set to 100%. The data represents means ± SEM of at least three independent experiments performed in triplicate. The difference between exposed and unexposed (clear histogram) cells was evaluated using non-parametric Kruskal-Walli's test. $p > 0.05$ = n.s; $p < 0.05$ = *; $p < 0.01$ = ** ; $p < 0.001$ = ** *; $p < 0.0001$ = ** ** .

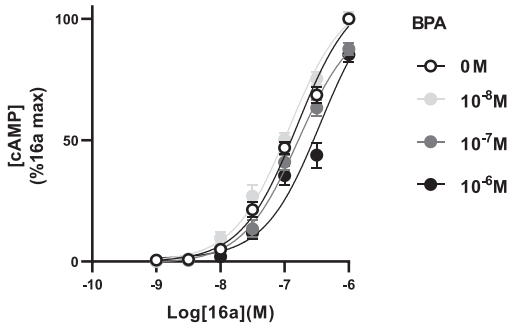

Concentration BPA (M)	0	10^{-8}	10^{-7}	10^{-6}
pEC_{50} (M)	6.79 ± 0.12	6.86 ± 0.25	6.81 ± 0.13	6.40 ± 0.42
Emax	100.00 ± 2.18	100.60 ± 2.42	87.50 ± 2.66 **	85.22 ± 3.19 **

Fig. 3. Effect of halogenated-derivatives BPA on 16a-stimulated cAMP production. CHO-FSHR-GLO cells were incubated with increasing concentrations of 16a in the presence of increasing concentrations of BPA. The maximum response to 16a was arbitrarily set at 100%. Data represented means ± SEM of three independent experiments performed in triplicate. Table represents efficacy (E_{max}) and potency (EC_{50}) of 16a on FSHR measured in different cAMP assay with different concentrations of BPA. Statistical analyses were performed with one-way Dunn's multiple comparisons test for the response in BPA-exposed compared with unexposed cells. $p > 0.05$ = n.s; $p < 0.05$ = *; $p < 0.01$ = ** ; $p < 0.001$ = ** *; $p < 0.0001$ = ** ** .

different halogen substitution patterns, or to size, number of halogen atoms, volume, and/or the degree of hydrophobicity of the compounds (Table S3). Indeed, based on their structural characteristics and physicochemical properties, several studies suggest that the effect of halogenated BPA derivatives on their molecular target dependent on the size, number and position of halogen atoms, and molecule's hydrophobicity [54-56]. Increased halogenation of the phenolic rings of BPA reduces the hormonal activity of halogenated derivatives towards ERα. The opposite is observed for PPARγ [57,58]. Molecular weight, volume and hydrophobicity of Br_xBPA compounds are correlated with increasing TRβ affinity [59]. On the other hand, the ERRγ transcriptional activity in the presence of halogenated BPA derivatives decreases with the increasing compound size and number of halogen atoms [56], and the presence of a halogen atom in the 2 or 2′ position increases cytotoxic effects of the compounds (Marques Dos Santos et al., 2024). Very recently, it has been shown that the hydrophobicity of halogenated BPA derivatives determines the degree of inhibition of aromatase activity [60]. Whatever the conditions tested, we did not observe any effect of Br_4BPA on the FSHR activity. It is possible that Br_4BPA, being the heaviest and most hydrophobic molecule within the tested group, was unable to adequately bind to the FSHR. In our study, the number of halogen atoms, molecular weight, volume and hydrophobicity did not seem to correlate with the inhibitory effect of the compound on the response to FSH. We suggest that it is the binding pose and the nature of the interactions (hydrogen or halogen bonds) between BPA or halogenated BPA derivatives and the receptor that determine the degree of inhibition of the

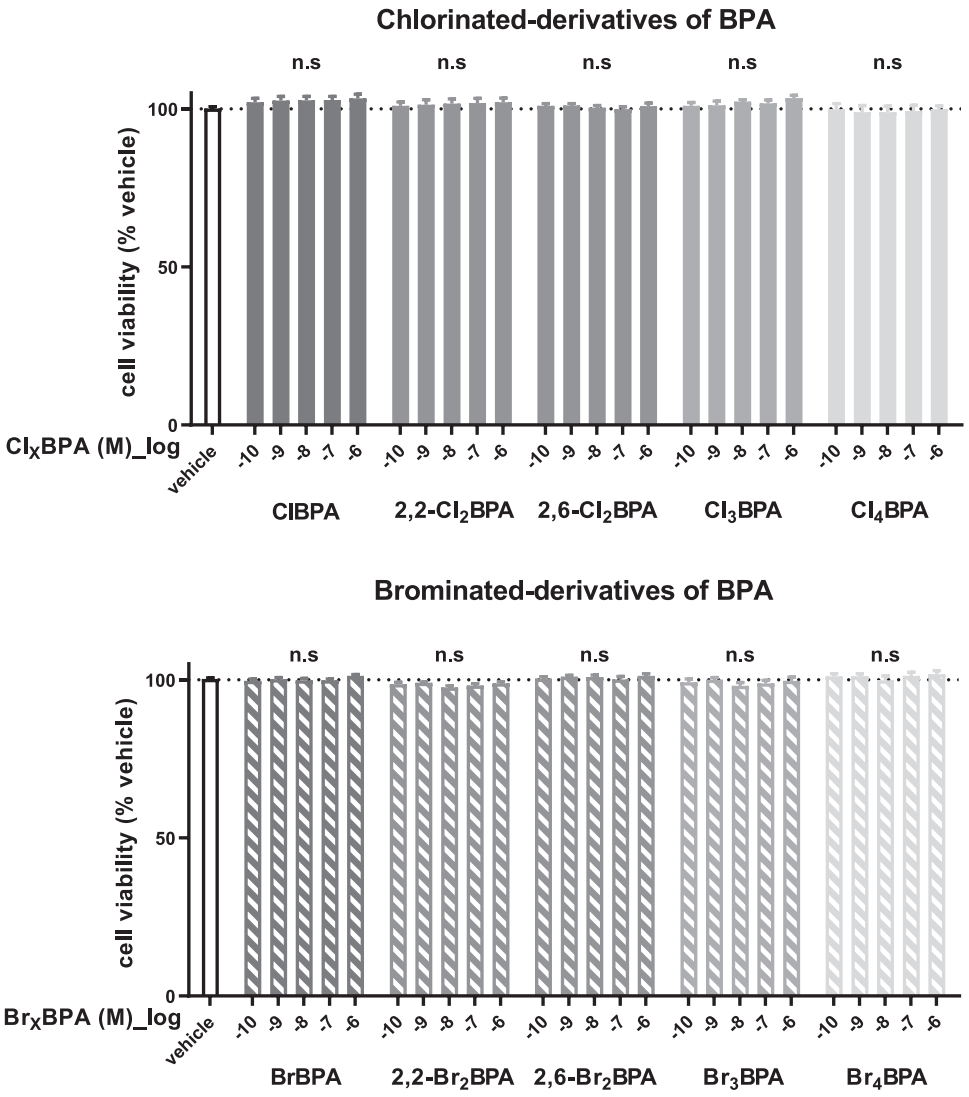

Fig. 4. Effect of halogenated-derivatives BPA on cellular viability. CHO-FSHR-GLO were incubated with increasing concentrations of halogenated BPA derivatives for 1 h. The results are expressed as percentage of viability compared to cells in absence of halogenated BPA derivatives (means ± SEM of three independent experiments performed in triplicate). The difference between exposed and unexposed cells was evaluated using non-parametric Kruskal-Walli's test. $p > 0.05$ = n.s; $p < 0.05$ = *; $p < 0.01$ = ** ; $p < 0.001$ = ** *; $p < 0.0001$ = ** ** .

hormonal response. Previous studies have also shown that Cl_xBPA compounds at low concentrations are agonists of the membrane estrogen receptor GPER1 [61,62]. No data on the interaction site of Cl_xBPA within GPER1 have been collected, whereas BPA and 2,2-bis(4-hydroxyphenyl)-dichloroethylene (BPC) have been shown to bind to the orthosteric site in the GPER transmembrane domain [63,64]. FSH interacts with the large extracellular N-terminal domain of its receptor, but low molecular weight ligands have been designed to bind to the FSHR transmembrane domain [65,66]. Moreover, we showed that the organochlorine pesticide, 1-chloro-4-[2,2,2-trichloro-1-(4-chlorophenyl)ethyl]benzene (p,p'DDT) binds in transmembrane domain of FSHR and positively modulates the FSH response [28]. We therefore hypothesize that the interaction site of halogenated BPA derivatives is in the receptor transmembrane domain, making FSHR a molecular target of BPA and its halogenated analogues.

3.2. Structural analysis of the chlorinated BPA derivatives and the FSHR transmembrane domain complexes

We focused on BPA as the group representative and addressed p,p'-DDT binding. The p,p'DDT consists of two phenyl rings associated with five chlorine atoms (Fig. 1). Both structures of BPA and p,p'DDT share the two phenyl rings but contain different halogen atoms and methyl and hydroxyl groups. FSH interacts with the large extracellular N-terminal domain of its receptor, at its transmembrane domain, FSHR has while the two allosteric sites (named major site and minor site) are located within its transmembrane domain. The major site is mainly formed by TM3-TM4-TM5-TM6-TM7, and the minor site by TM1-TM2-TM7 [67]. Previously, p,p'DDT was observed to bind between TM2, TM3 and TM7, in the vicinity of $T449^{TM3}$ and $H615^{TM7}$ [28]. The then-used FSHR model was built upon a rhodopsin template (PDB ID: 3C9L) which exhibits a widened minor site due to a kink in TM2 [68]. However, our updated homology model was based upon the LHCGR template [35] with a higher sequence identity to FSHR (70% in the transmembrane domain as compared to 21% for rhodopsin), and it did not feature the TM2 kink. Furthermore, ECL2, which obstructs the part of the site, was anchored to TM3 by a disulphide bridge in the new model and was thus limits the loop flexibility. The p,p'-DDT binding site was therefore re-evaluated in this study and the resulting docking poses showed that the cavity between the TM2, TM3 and TM7 was inaccessible for compounds of interest.

BPA and p,p'DDT were docked into FSHR minor site between TM1,

Table 1
Maximum effect observed for each compound tested with the associated concentration (C_{Emax}) on the FSHR activity.

	FSH 3 IU/mL								FSH 0.03 IU/mL							
Compound	C_{Emax} of compound (M)	Maximal effect (% of inhibition ± SEM)	Lower 95% CI of mean	Upper 95% CI of mean	%CV	$n_{replicates}$	$n_{experiments}$	p_value	C_{Emax} of compound (M)	Maximal effect (% of inhibition ± SEM)	Lower 95% CI of mean	Upper 95% CI of mean	%CV	$n_{replicates}$	$n_{experiments}$	p_value
BPA	1E−06	**29.82 ± 5.54**	17.47	42.17	61.65	11	4	n.a	1E−09	**42.36 ± 4.41**	32.53	52.20	34.55	11	4	n.a
ClBPA	1E−06	25.41 ± 4.35	15.58	35.24	54.08	10	4	0.5	1E−07	**26.12 ± 5.85**	13.25	38.99	77.55	12	4	0.03
2,2-Cl_2BPA	1E−06	19.25 ± 6.40	5.16	33.33	115.2	12	4	0.2	1E−07	32.79 ± 4.62	22.61	42.96	48.83	12	4	0.1
2,6-Cl_2BPA	n.a	n.a	n.a	n.a	n.a	n.a	n.a	n.a	1E−07	27.18 ± 12.77	- 2.28	56.63	141.00	9	3	0.2
Cl_3BPA	1E−06	24.63 ± 7.14	8.90	40.36	100.5	12	4	0.5	1E−07	**29.28 ± 3.59**	21.38	37.17	42.46	12	4	0.03
Cl_4BPA	1E−09	27.95 ± 6.97	12.60	43.29	86.42	12	4	0.8	1E−08	**26.57 ± 3.21**	19.51	33.63	41.82	12	4	0.009
BrBPA	1E−06	19.83 ± 4.90	8.53	31.12	74.15	9	3	0.1	n.a	n.a	n.a	n.a	n.a	n.a	n.a	n.a
2,2-Br_2BPA	n.a	n.a	n.a	n.a	n.a	n.a	n.a	n.a	1E−10	**27.04 ± 5.68**	13.94	40.14	63.03	9	3	0.04
2,6-Br_2BPA	n.a	n.a	n.a	n.a	n.a	n.a	n.a	n.a	1E−09	**22.46 ± 3.04**	15.44	29.48	40.66	9	3	0.001
Br_3BPA	1E−07	17.44 ± 6.63	2.16	32.73	114	9	3	0.1	1E−07	**22.42 ± 4.28**	12.54	32.30	57.32	9	3	0.004
Br_4BPA	n.a	n.a	n.a	n.a	n.a	n.a	n.a	n.a	n.a	n.a	n.a	n.a	n.a	n.a	n.a	n.a

Table 1 lists the maximum effect (expressed as a percentage of the inhibition of response to FSH) observed for each compound tested with the associated concentration (C_{Emax}), the percentage of confidence interval (CI) and the statistical results for maximum effect comparison with BPA. Statistical analyses were performed with Welch's test for the difference between BPA effects compared to halogenated BPA derivatives. CV = Coefficient of variation; n.a= not applicable

TM2, and TM7 and assessed for stability by monitoring their RMSD values and interactions with the pocket residues (Fig. 5). Generally, BPA exhibited stable binding in the $FSHR_{inact}$, whereas it tended to leave the binding site if the receptor was in the active conformation. On the other hand, p,p'-DDT exhibited more stable binding in $FSHR_{act}$, with a better overall pose agreement across repeats. As the docking poses were built from the ground up for each FHSR conformation, we cannot exclude the possibility that the observed higher stability was a consequence of a better ligand pose that was discovered during the docking protocol, rather than the effect of FSHR conformation. Molecular dynamics simulations also showed that the FSHR conformation remained for the most part unchanged regardless of the identity of the ligand. This was in line with the experimental observation that BPA, halogenated BPA derivatives, and p,p'-DDT did not change the basal activity of FSHR. Jointly, these data suggest that the compounds do not directly modify the energy landscape nor the conformational population ratios of FSHR. Instead, BPA and its halogen derivatives affect the FSHR response to FSH specifically by hindering signal transduction.

An interesting observation was the difference between the binding mode of BPA in $FSHR_{inact}$ and p,p'DDT in $FSHR_{act.}$ For BPA in $FSHR_{inact}$, one phenol pointed towards the extracellular medium, while the other pointed towards TM2. For p,p'DDT in $FSHR_{act}$, one of the p-chlorophenyl groups was oriented towards the intracellular milieu and was located between TM1 and TM7, while the other p-chlorophenyl group was pointing towards the extracellular medium. The interaction of BPA with GPER at the site constituting the TM2-TM6-TM7 helices also occurred via hydrogen bonds. BPA is a GPER agonist (and not an allosteric modulator, as is the case for FSHR) [64]. The difference in BPA activity with regards to the receptor can be explained by the ligand being positioned at different binding sites and consequently having a different impact on signal transduction.

The protein-ligand interaction analysis identified 10 main interaction partners of BPA and p,p'DDT in FSHR, sharing 9 of them. (Fig. 6). BPA was stabilised in the binding site with both hydrogen bonds ($I418^{TM2}$, $D422^{ECL1}$, $K608^{ECL3}$ and $S605^{TM7}$) and hydrophobic interactions ($Y362^{TM1}$, $L365^{TM1}$, $R366^{TM1}$, $I369^{TM1}$, $K608^{ECL3}$, $I609^{TM7}$, and $V612^{TM7}$). Conversely, the stability of p,p'DDT primarily depended on hydrophobic interactions ($Y362^{TM1}$, $L365^{TM1}$, $R366^{TM1}$, $I369^{TM1}$, $I418^{TM2}$, $D422^{ECL1}$, $K608^{TM7}$ and $V612^{TM7}$) with the receptor. Recently published cryo-EM structures of FSHR in active and inactive conformation [69] offered structural details of the mechanism of FHSR signal transduction. Based on the structures, FSH binding to the FSHR extracellular domain induces an almost 50° rotation within the domain, bringing the hinge loop into the interacting distance from the transmembrane domain. This motion also sandwiches the conserved P10 region (residues 353–362), which functions as a tethered intermolecular agonist [70], between the extracellular domain and the transmembrane domain. In this active conformation, P10 forms hydrogen bonds with R366 on TM1, S605 and K608 on TM7, and Q437 on ECL1 [69]. Additionally, the contact surface is stabilised with hydrophobic interactions with L365, V421, I418, W436 ECL1, and V612 on TM7. Y362 is a part of P10 and presumably forms a hydrogen bond with K606. It is notable that almost all P10 interacting partners also featured as residues involved in the binding of investigated allosteric modulators. We hypothesise that BPA and halogenated derivatives disrupt P10 interactions with the transmembrane domain by occupying the minor site of FHSR, thus preventing stable P10 interaction with transmembrane domain, and consequently hindering signal transduction from extracellular domain to transmembrane domain. The FSHR models used for docking and simulations excluded extracellular domain and the hinge region, as our focus was on the allosteric sites located in transmembrane domain. However, in the active state of FHSR, the top part of the minor site is bordered by P10 [69], which forms an upper surface of the pocket. Presumably, inclusion of the whole extracellular domain would have helped identify P10 residues interacting with the ligands. However, the interface between extracellular domain and transmembrane domain was

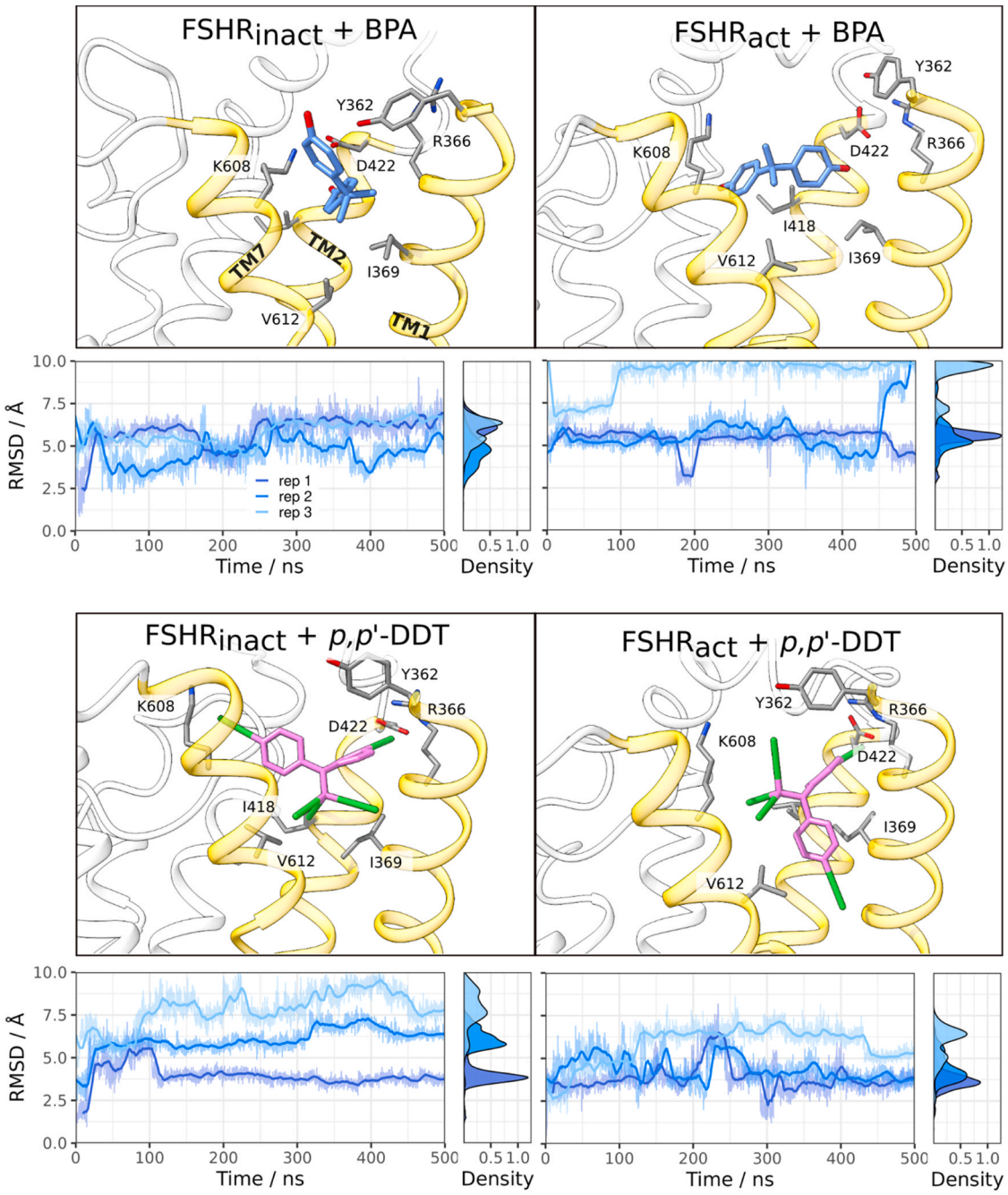

Fig. 5. Most populated poses for each FSHR conformation and ligand pair. TM1, 2 and 7 are shown in yellow ribbons and labelled in the first figure. Ligands are shown in licorice, with carbon atoms in blue for BPA and in violet for *p,p'*-DDT. Interacting residues are shown in thinner licorice representation and labelled accordingly. Under the pose figures, a pair of plots show RMSD values of the corresponding ligand as a function of time and density. RMSD values were calculated for each repeat and with the starting docked poses as references.

bound to be disrupted or modified by the addition of allosteric modulators, and the identification of the correct docking poses would therefore be less likely if we would have considered the full static structures for the docking study.

To analyse putative interactions between the ligands and the transmembrane domain, we produced several FSHR mutants in TM1 and TM7 (R366A, Y362A and S605A). These residues were chosen based on the criteria of i) conservation among the other different glycoprotein hormone receptors (LHCGR and TSHR), ii) high interaction ratio between the ligands and the receptor in molecular dynamics simulations, iii) interaction contributions to the binding energy, obtained from molecular dynamics simulations (Fig. S3), and iv) their ability to maintain a response to FSH when mutated in alanine (Fig. S4). As the 3.10^{-2} IU/mL FSH induced-cAMP production was very low for FSHR mutants, only 3 IU/mL FSH induced-responses were studied on mutated FSHR for each key residue. Even though the alanine substitution of $Y362^{TM1}$ maintained the BPA inhibiting activity on FSH signalling, the alanine substitution of $R366^{TM1}$ or $S605^{TM7}$ abolished this BPA effect (Fig. 7). These results therefore demonstrated that BPA binds the FSHR minor site, and that $R366^{TM1}$ and $S605^{TM7}$ are crucial for stabilising the ligand in the binding site. Interestingly, even though simulations suggested that $Y362^{TM1}$ stabilised the ligand binding through π-π stacking interactions (Fig. S3), mutagenesis experiments showed that the aromatic ring was not crucial for maintaining the ligand binding to FHSR. The two highest

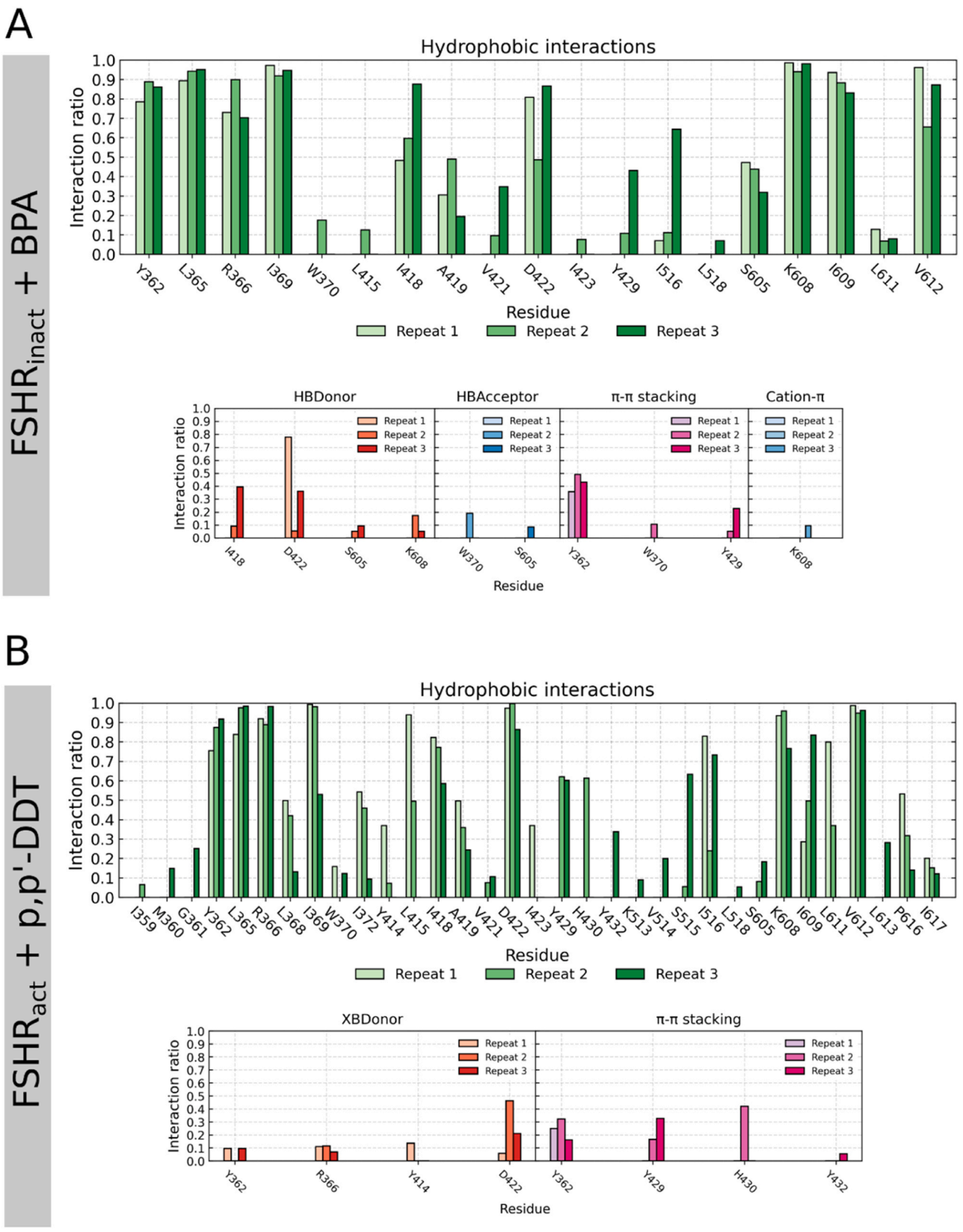

Fig. 6. Interactions occurring during the course of molecular dynamic simulations between (A) BPA and FSHR$_{inact}$, and (B) p,p′-DDT and FSHR$_{act}$. The plots show receptor residues participating in hydrophobic interactions, hydrogen bonding (HB), π-π stacking, cation-π interactions, and halogen bonds (XB). The ratios signify a fraction of analyzed simulation frames in which the interactions are detected. Interactions occurring less than 5% of simulation time are not shown.

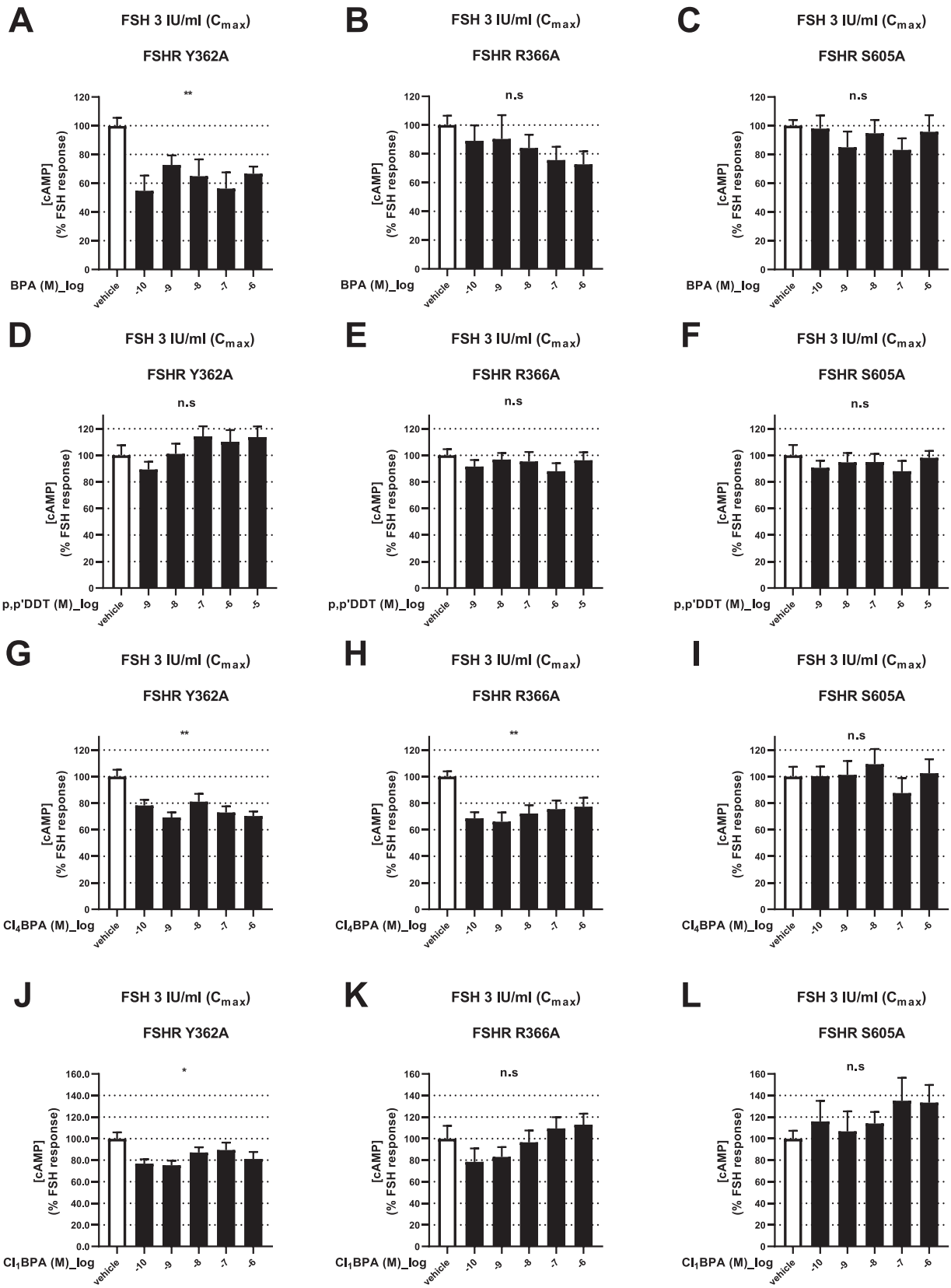

Fig. 7. Effect of halogenated-derivatives BPA on mutants FSHR. FSHR Y362A (A,D,G,J), R366A (B,E,H,K) and S605A (C, F, I, L) transiently expressed in CHO cells and stimulated with 3 IU/mL FSH with or without increasing concentrations of BPA (A,B,C), p,p′DDT (D,E,F), Cl_4BPA (G,H,I) and ClBPA (J,K,L). Data represented means ± SEM of six independent experiments performed in triplicate. The maximum response to FSH was arbitrarily set to 100. The difference between exposed and unexposed cells was evaluated using non-parametric Kruskal-Walli's test. $p > 0.05$ = n.s; $p < 0.05$ = *; $p < 0.01$ = ** ; $p < 0.001$ = ** *; $p < 0.0001$ = ** ** .

binding energy contribution residues, D422^{ECL1} and K608^{ECL3} (Fig. S3), could not be mutated into alanine, as these mutants cannot appropriately respond to the FSH stimulus [71,72]. The Y362A, R366A and S605A FSHR mutants did not display any sensitivity to p,p′-DDT in the presence of 3 IU/mL FSH (Fig. 7). This result clearly endorses the hypothesis that p,p′-DDT binds the FSHR minor site through Y362^{TM1}, R366^{TM1}, and S605^{TM7} interactions. *In silico* data showed a halogen bond between a chlorine atom of p,p′-DDT and R366^{TM1} of FSHR, hydrophobic bonds between the ligand trichloroethane group and S605^{TM7}, Y362^{TM1} and R366^{TM1}, and a π-π interaction between the phenyl group of p,p′-DDT and the aromatic ring of Y362^{TM1} (Fig. S3). While the Y362A and R366A mutants did not alter the Cl_4BPA effect, the S605A mutation abolished the Cl_4BPA inhibitory effect on the FSH response (Fig. 7). Alanine substitution of Y362^{TM1} maintained the ClBPA inhibiting activity on FSH signalling, while the alanine substitution of R366 or S605 abolished it (Fig. 7). The FSH induced responses of FSHR mutant in the presence of halogenated BPA showed that both tested compounds bind to the minor site, but the main stabilising interactions differ regarding the position of the chloride atoms. Indeed, mutant response data showed that both BPA and ClBPA are stabilised by R366^{TM1} and S605^{TM7}, but not by Y362^{TM1}, suggesting a similar binding mode. On the other hand, Cl4BPA binding was disrupted only by alanine substitution of S605A, which implies different compounds orientation within the binding site.

FSHR/BPA or FSHR/p,p′-DDT molecular dynamics simulations were analyzed by monitoring multiple conserved crucial motifs for receptor activation. During activation, the ionic lock between R467^{TM3} and D567^{TM6} is broken, which allows for TM6 to kink outwards on the intracellular side of the receptor. BPA binding did not change the receptor dynamics, whereas p,p′-DDT binding stabilized the active conformation as measured by monitoring the conserved motifs important for receptor activation (Fig. 8). Thus, the p,p′DDT binding to FSHR would increase the receptor affinity for 16a or FSH, resulting in increased potency. In contrast, BPA binding to FSHR may lower the receptor affinity for 16a or FSH, leading to magnitude reduction of the FSHR response. Furthermore, FSHR basal activity was not modified by BPA, suggesting that it does not inhibit FSHR activation but more specifically signal transduction. Therefore, halogenated BPA derivatives had negative allosteric modulator activity toward FSHR signalling and could be considered as an emerging group of endocrine-disrupting chemicals.

3.3. Concentrations and detection rate of halogenated BPA derivatives in human biological fluids: health risk assessment

The quantitative in vitro to in vivo extrapolation model is recommended as a new approach to evaluate the human health risk [73]. The Hazard Quotient (HQ) model is a simple model based on a direct comparison between a concentration measured in human biological matrices (reflecting actual exposure) and a lowest effective concentration (LOEC) established in vitro. The HQ model makes it possible to establish a clear relationship between current exposure and concentration levels associated with known adverse effects. To compare the halogenated derivatives-concentrations which have significant in vitro effect on FSH signalling with those measured in human biological matrices (blood and urine), a literature review was performed. Only one study assessed the Cl_4BPA concentration in 181 pregnant women serum (0.14 μg/L or 0.38 nM) [43] while five studies assessed the Br_4BPA concentration in the serum of healthy individuals (mean = 2.44 μg/L or 6.7 nM) [44-47, 43] (Table S2). As there are no data on blood concentrations of Cl_xBPA found in the blood of healthy adults, we therefore focused on urine concentrations measured in healthy adults (Table 2). All compounds were detected at an equivalent detection rate of 35 to 59%, and the mean urinary concentrations of BPA and Br_4BPA are equivalent (in the nanomolar range) and 10-fold higher than those of other halogenated derivatives. As it is being used as a flame retardant produced in massive quantities, Br_4BPA is frequently detected in human tissues with similar concentrations to BPA [74].

Halogenated BPA derivatives are detected in drinking water [24,10, 41]. The concentrations of BPA are 10 to 10 000-fold higher than those of the halogenated derivatives. *In vitro*, we show that for a concentration of 10^{-10} M, the halogenated BPA derivatives significantly reduce the response to FSH, except for Br_4BPA (which exhibits no effect). In drinking water, the maximum concentration found for ClBPA is 26.7 ng/L (i.e., 10^{-10} M) [41], for Cl_2BPA is 100 ng/L (i.e., 3.4×10^{-10} M), for BrBPA is 43.2 ng/L (i.e., 10^{-10} M) and for Br_2BPA is 83.2 ng/L (i.e., 2×10^{-10} M) [24] Thus, in some drinking water samples, the concentrations for these four compounds can have a significant effect on FSH signalling, suggesting that the environmental levels of halogenated BPA derivatives may be of concern, and that their potential health risks cannot be overlooked. The maximum concentrations for the other halogenated BPA derivatives are lower than the experimentally defined LOEC (Table S4).

According to our in vitro data, 10^{-10} M halogenated BPA derivatives significantly reduced the response to FSH. Based on the reported human exposure level and LOEC on FSHR activity obtained in our study, the potential health risk of Cl_xBPA was evaluated (Table 2). Hazard quotient values are higher than 1 and therefore suggest that the current exposure levels may be of concern. However, our study model has limitations. First, in human health risk assessments, the human exposure concentration must be similar to the in vitro adverse effect concentration [75]. It is therefore inaccurate to compare the in vitro effect concentration to the urinary concentration, as the latter ones are not equal to the concentration in the target tissue (in this case, the gonads). For this reason, the in vivo concentration in the gonads should have been predicted using Physiologically Based Pharmacokinetic (PBPK) modelling: this bioinformatics approach is based on the mechanisms that drive the absorption, distribution, metabolism and excretion (ADME) of chemicals in the body as a function of the inter-relationships between the main physiological, biochemical and physicochemical determinants [76]. However, there is currently no toxicokinetic data on halogenated BPA derivatives [23]. Our results offer a preliminary risk assessment of a potential health risk, but do not allow in vitro effects to be extrapolated to in vivo effects. Secondly, BPA is rapidly metabolized to the biologically inactive glucuronated or sulfated conjugates [77]. Glucuronoconjugation and sulfoconjugation of Cl_4BPA and Br_4BPA have been demonstrated as well [78]. We can therefore hypothesize that their excretion is similar to BPA [23], while few non-conjugated compounds are excreted in urine, which is therefore not a good indicator of exposure [47].

The approximative comparison of Cl_xBPA blood levels from biomonitoring data with those reducing FSH signalling may be essential in human health risk assessment. The most in vitro inhibitory Cl_xBPA concentrations ranged from 10^{-8} to 10^{-7} M, although a significant effect was observed already at 10^{-10} M. Only two studies have quantified Cl_xBPA in blood: one from 10 patients suffering from end-stage renal disease [42], and one focused only on Cl_4BPA [43], and the reported 10^{-10} M urinary concentration is in the same range than Cl_xBPA inhibitory concentrations. Regarding Br_4BPA, which did not disrupt in vitro FSH signalling in this work, two studies have measured total Br_xBPA in breast milk [79,80], and Br_4BPA concentrations were estimated in blood (2.44 ± 2.80 μg/L [44-47,43] and urine (0.62 ± 0.81 μg/L [47,50,51].

Halogenated BPA derivatives also target nuclear receptors: peroxisome proliferator-activated receptors (PPARs, with a LOEC of 10^{-5} to 10^{-6} M) [55,78], or estrogen receptors (ERs, with a LOEC of 10^{-8} to 10^{-7} M) [78], and steroidogenesis enzymes such as 11β-hydroxysteroid dehydrogenase 1 (11βHSD1, with a LOEC of 10^{-6} M) [81] or 3β-hydroxysteroid dehydrogenase (3βHSD, with a LOEC of 10^{-6} M) [82].

In addition, after a 24 h exposure, halogenated BPA derivatives are cytotoxic in concentrations greater than 10^{-6} M [8,83]. When comparing the halogenated BPA derivatives LOECs for these targets with

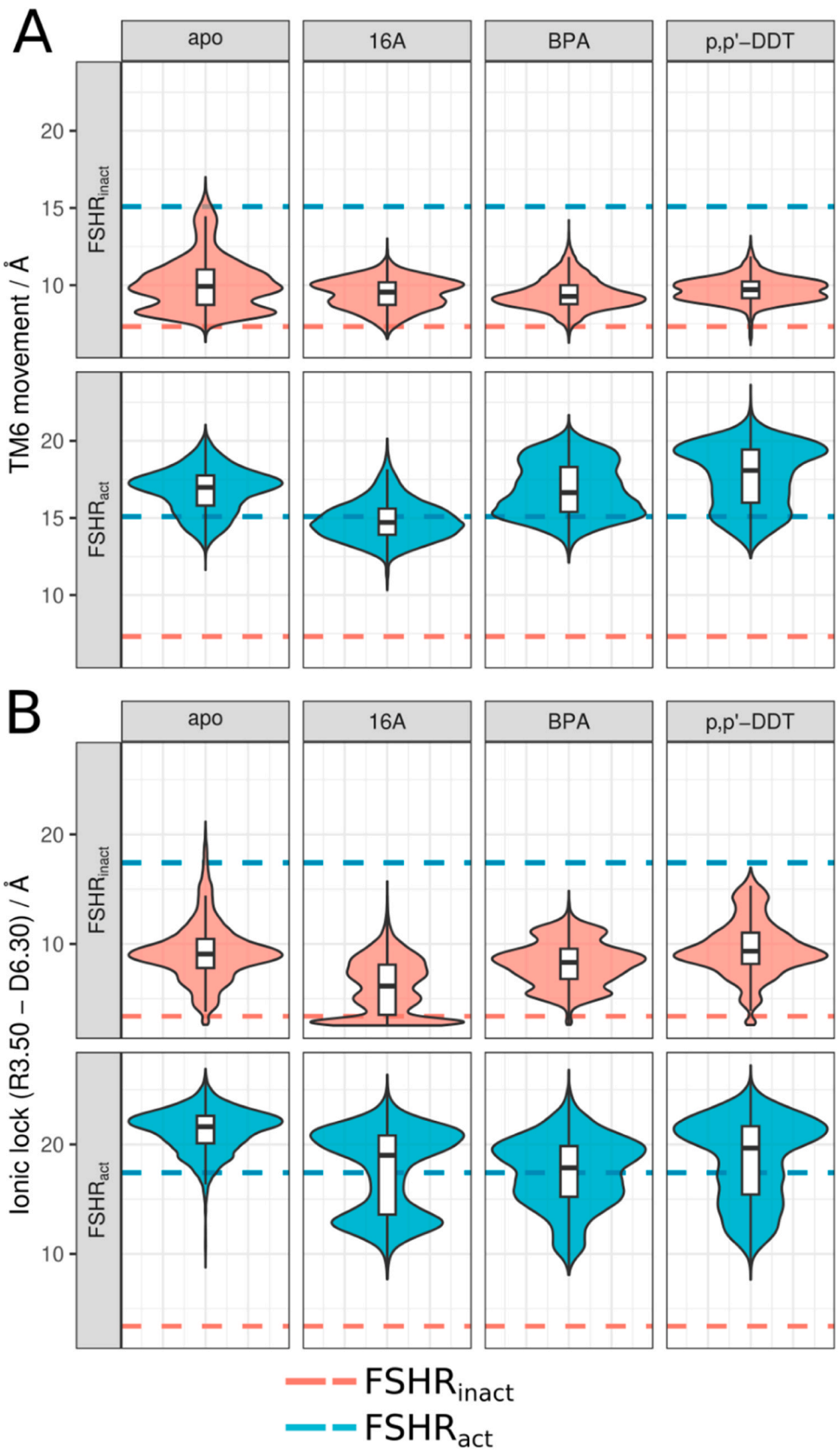

Fig. 8. Measures of FSHR activation in molecular dynamic simulations for all systems. Measures shown as violin plots and overlaid with barplots. Reference values for inactive and active conformations were measured from the homology models and shown in dashed lines. (A) TM6 movement was measured by monitoring the distance between the Cα atoms of R467^{TM3} and A571^{TM6}. Increased distance is expected in the activated receptor conformations. (B) Ionic lock was calculated by measuring the minimum distance between the polar atoms of the side chains of R467^{TM3} and D567^{TM6}. Values across repeats were combined in a single density plot.

Table 2
Exposure levels of halogenated derivatives-BPA in human urine and health risk assessment evaluation.

Molecule	Detection rates (%) - **Mean detection rates ± SD (%)**	Urinary concentration (µg/L) - **Mean urinary concentration ± SD (µg/L) [nM]** [#]	LOEC (nM)	Hazard Quotient	References
BPA	25[a]; 24[b]; 60[c]; 100[d]; 97[e]	0.62[a]; 0.076[b]; 0.51[c]; 3.75[d]; 0.70[e]	**0.1**	**49 600**	Xu et al., [51][a]; [50][b]; [48][c]; [27][d];
	59 ± 33	**1.13 ± 1.48 [4.96]**			
Cl_1BPA	70[c]; 90[d]; 16[e]	0.032[c]; 0.083[d]; 0.055[e]	**0.1**	**2 200**	[49][e];[47][f]
	59 ± 31	**0.06 ± 0.03 [0.22]**			
Cl_2BPA	70[c]; 19[e]	0.017[c]; 0.048[e]	**0.1**	**1 100**	
	45 ± 36	**0.03 ± 0.02 [0.11]**			
Cl_3BPA	70[c]; 19[e]	0.035[c]; 0.047[e]	**0.1**	**1 200**	
	43 ± 25	**0.04 ± 0.01 [0.12]**			
Cl_4BPA	36[a]; 24[b]; 40[c]	0.073[a]; 0.03[b]; 0.03[c]	**0.1**	**1 200**	
	35 ± 8	**0.04 ± 0.02 [0.12]**			
BrBPA	n.a	n.a	**0.1**	n.a	
Br_2BPA	n.a	n.a	**0.1**	n.a	
Br_3BPA	n.a	n.a	**0.1**	n.a	
Br_4BPA	16[a]; 4[b]; 87 [f]	1.56[a]; 0.12[b]; 0.19 [f]	n.e	n.a	
	35 ± 45	**0.62 ± 0.81 [1.15]**			

HQ ≤ 1 indicates an absence of risk for the endpoint considered, whereas HQ ≥ 1 indicates exposure may be regarded as being of concern.
LOEC = the lowest effective concentration; SD = standard deviation; n.d = no data; n.a = not applicable; n.e = no effect
[#] Mean urinary concentrations based on a literature review and converted to nM in brackets

current exposure levels, we conclude that FSHR is preferentially inactivated. At the urinary concentrations described (between 10^{-10} and 10^{-9} M), we hypothesise that exposure to halogenated BPA derivatives modifies the activity of steroidogenesis enzymes and hormone receptors, rather than induce a cytotoxic effect. The reduction in FSH/FSHR signalling results in adverse effects on reproductive function leading to infertility [84], the in vitro FSH response decrease in the presence of BPA or its halogenated derivatives may have deleterious in vivo effects. Our results provide mechanistic evidence for the negative effect of BPA on follicular recruitment as supported by human [85] and animal data [86-88]. Moreover, the reverse association between BPA levels in serum or follicular fluid and exogenous FSH-ovarian response has been shown in women undergoing medically assisted reproduction [89,90].

4. Conclusion

Thanks to the interdisciplinary strategy, we demonstrate, for the first time, that peptide hormone receptor FSHR as a new potential target of halogenated BPA derivatives which are part of the human exposome via drinking water disinfection. At low concentrations (100pM), the compounds show negative allosteric modulation of FSHR which is based on signal interruption between the FSH-bound extracellular domain and the transmembrane domain, resulting in a reduced cAMP response up to 42.36% by BPA, up to 32.79% by chlorinated BPA derivatives and up to 27.04% by brominated BPA derivatives. This mode of action differs from previous study showing disruptions of FSH receptors expression or FSH secretion [91]. The comparison of the LOEC (0.1 nM) established by in vitro approaches with concentrations found in human fluids and representing the exposure of individuals suggests that the potential health risk of halogenated BPA derivatives cannot be overlooked. Our study provides new evidence suggesting that halogenated BPA derivatives are potential endocrine disruptors. Halogenated BPA derivatives have been detected in human biological samples, but above all in drinking water (a vital resource for humans), which means that the general population may be affected by these compounds. It is therefore urgent to perform a complete risk analysis, including a study of their toxicokinetics (ADME), and to study their effects on other elements of the endocrine system to complete the lack of knowledge about their endocrine disrupting effect. Comparison of the LOEC of halogenated BPA derivatives toward the different identified targets with known exposure levels show that the GPCR (FSHR or GPER) are preferentially activated. In order to characterise the toxicological and/or endocrine disrupting profile of halogenated BPA derivatives, future studies should include analysis of their effects on GPCR signalling, in addition to their effects on nuclear receptor signalling and the activity of steroidogenesis enzymes. Given the lack of in vivo data regarding the consequences of their exposure on reproductive function, the multidisciplinary approach used here represents an alternative and a preliminary step in the assessment of halogenated BPA derivatives. This experimental approach could be used to assess toxicological changes after the drinking water disinfection stage and to estimate a range of concentrations of halogenated BPA derivatives that are safe for human health. This would guarantee the safety of disinfected drinking water. To conclude, our study revealed a novel molecular mechanism for better understanding the mode of action of halogenated BPA derivatives, providing new insights into their exposure risk.

Environmental implication

BPA is a plastic additive that is ubiquitous in the environment. Halogenated BPA derivatives are formed during disinfection treatment of drinking water or are synthetized to be used as flame retardants. This study shows that halogenated derivatives, like BPA, inhibit the FSH response by interacting with the transmembrane domain of the FSH receptor, and do so in concentrations that are relevant to humans. The FSH hormone plays a critical role in reproductive function (gametogenesis and steroidogenesis) and fertility. Halogenated derivatives of BPA act as endocrine disruptors. Comparison of in vitro effects with human biomonitoring data suggests that current levels of exposure may give cause for concern, and that the potential health risk cannot not be neglected.

Ethics approval

Not applicable.

Funding

LZ, DHH, LRK and BS acknowledge Novo Nordisk Foundation (Grant No. NNF18OC0032608) for the use of computational resources and access to computational infrastructure at Centre for Scientific Computing Aarhus (CSCAA). LZ acknowledges Lundbeck Foundation Experiment (R346-2020-1944) research grant.

CRediT authorship contribution statement

Ditlev Høj Hansen: Data curation. **Mathilde Munier:** Writing – review & editing, Writing – original draft, Supervision, Project administration, Methodology, Investigation, Formal analysis, Data curation, Conceptualization. **Lisbeth Kjølbye:** Formal analysis. **Paul Sibilia:** Data curation. **Hélène Tricoire-Leignel:** Writing – review & editing. **Birgitt Schiøtt:** Supervision. **Valentine Suteau:** Writing – review & editing, Data curation. **Pascal Carato:** Writing – review & editing. **Lorena Zuzic:** Writing – original draft, Formal analysis, Data curation. **Patrice**

Rodien: Writing – original draft, Supervision. **Louis Gourdin:** Data curation. **Claire Briet:** Visualization. **Mickael Thomas:** Data curation. **Eric Bourdeaud:** Data curation.

Declaration of Competing Interest

The authors declare the following financial interests/personal relationships which may be considered as potential competing interests: Zuzic Lorena reports equipment, drugs, or supplies was provided by Novo Nordisk Foundation. Zuzic Lorena reports financial support was provided by Lundbeck Foundation. If there are other authors, they declare that they have no known competing financial interests or personal relationships that could have appeared to influence the work reported in this paper.

Data Availability

Data will be made available on request.

Acknowledgments

We thank Manon Doumas (Poitiers University) for the synthesis of halogenated derivatives of bisphenol A. We thank Lucy Kate Ladefoged for her advice and support of the *in silico* part of this research.

Consent to participate

Not applicable.

Consent for publication

Not applicable.

Code availability

Not applicable.

Appendix A. Supporting information

Supplementary data associated with this article can be found in the online version at doi:10.1016/j.jhazmat.2024.135619.

References

[1] Pivnenko, K., Laner, D., Astrup, T.F., 2018. Dynamics of bisphenol A (BPA) and bisphenol S (BPS) in the European paper cycle: Need for concern? Resour Conserv Recycl 133, 278–287. https://doi.org/10.1016/j.resconrec.2018.01.021.
[2] Michałowicz, J., 2014. Bisphenol A–sources, toxicity and biotransformation. Environ Toxicol Pharm 37, 738–758. https://doi.org/10.1016/j.etap.2014.02.003.
[3] Gore, A.C., Chappell, V.A., Fenton, S.E., et al., 2015. EDC-2: the Endocrine Society's Second Scientific Statement on Endocrine-Disrupting Chemicals. Endocr Rev 36, E1–E150. https://doi.org/10.1210/er.2015-1010.
[4] Palsania, P., Singhal, K., Dar, M.A., Kaushik, G., 2024. Food grade plastics and Bisphenol A: associated risks, toxicity, and bioremediation approaches. J Hazard Mater 466, 133474. https://doi.org/10.1016/j.jhazmat.2024.133474.
[5] An, R., Liu, J., Chu, X., et al., 2024. Polyamide 6 microplastics as carriers led to changes in the fate of bisphenol A and dibutyl phthalate in drinking water distribution systems: The role of adsorption and interfacial partitioning. J Hazard Mater 476, 134997. https://doi.org/10.1016/j.jhazmat.2024.134997.
[6] Gallard, H., Leclercq, A., Croué, J.-P., 2004. Chlorination of bisphenol A: kinetics and by-products formation. Chemosphere 56, 465–473. https://doi.org/10.1016/j.chemosphere.2004.03.001.
[7] Yamamoto, T., Yasuhara, A., 2002. Chlorination of bisphenol A in aqueous media: formation of chlorinated bisphenol A congeners and degradation to chlorinated phenolic compounds. Chemosphere 46, 1215–1223. https://doi.org/10.1016/s0045-6535(01)00198-9.
[8] Marques Dos Santos, M., Li, C., Jia, S., et al., 2024. Formation of halogenated forms of bisphenol A (BPA) in water: resolving isomers with ion mobility - mass spectrometry and the role of halogenation position in cellular toxicity. J Hazard Mater 465, 133229. https://doi.org/10.1016/j.jhazmat.2023.133229.
[9] Soltermann, F., Abegglen, C., Götz, C., von Gunten, U., 2016. Bromide sources and loads in swiss surface waters and their relevance for bromate formation during wastewater Ozonation. Environ Sci Technol 50, 9825–9834. https://doi.org/10.1021/acs.est.6b01142.
[10] Doumas, M., Rouillon, S., Venisse, N., et al., 2018. Chlorinated and brominated bisphenol A derivatives: synthesis, characterization and determination in water samples. Chemosphere 213, 434–442. https://doi.org/10.1016/j.chemosphere.2018.09.061.
[11] Li, C., Wang, Z., Yang, Y.J., et al., 2015. Transformation of bisphenol A in water distribution systems: a pilot-scale study. Chemosphere 125, 86–93. https://doi.org/10.1016/j.chemosphere.2014.11.047.
[12] Wang, Y.-X., Cui, Y.-Y., Zhang, Y., Yang, C.-X., 2022. Synthesis of reusable and renewable microporous organic networks for the removal of halogenated contaminants. J Hazard Mater 424, 127485. https://doi.org/10.1016/j.jhazmat.2021.127485.
[13] Kuo, C., Kuo, D.T.F., Chang, A., et al., 2022. Rapid debromination of tetrabromobisphenol A by Cu/Fe bimetallic nanoparticles in water, its mechanisms, and genotoxicity after treatments. J Hazard Mater 432, 128630. https://doi.org/10.1016/j.jhazmat.2022.128630.
[14] Li, X., Lu, S., Zhang, G., 2023. Three-dimensional structured electrode for electrocatalytic organic wastewater purification: Design, mechanism and role. J Hazard Mater 445, 130524. https://doi.org/10.1016/j.jhazmat.2022.130524.
[15] Guo, E., Zhao, L., Li, Z., et al., 2024. Biodegradation of bisphenol A by a *Pichia pastoris* whole-cell biocatalyst with overexpression of laccase from *Bacillus pumilus* and investigation of its potential degradation pathways. J Hazard Mater 474, 134779. https://doi.org/10.1016/j.jhazmat.2024.134779.
[16] Wang, X., Wang, Z., Su, J., et al., 2024. Simultaneous removal of calcium, phosphorus, and bisphenol A from industrial wastewater by *Stutzerimonas* sp. ZW5 via microbially induced calcium precipitation (MICP): Kinetics, mechanism, and stress response. J Hazard Mater 473, 134700. https://doi.org/10.1016/j.jhazmat.2024.134700.
[17] Sunday, O.E., Bin, H., Guanghua, M., et al., 2022. Review of the environmental occurrence, analytical techniques, degradation and toxicity of TBBPA and its derivatives. Environ Res 206, 112594. https://doi.org/10.1016/j.envres.2021.112594.
[18] Arbeli, Z., Ronen, Z., 2003. Enrichment of a microbial culture capable of reductive debromination of the flame retardant tetrabromobisphenol-A, and identification of the intermediate metabolites produced in the process. Biodegradation 14, 385–395. https://doi.org/10.1023/a:1027304222436.
[19] Huang, Q., Liu, W., Peng, P., Huang, W., 2013. Reductive dechlorination of tetrachlorobisphenol A by Pd/Fe bimetallic catalysts. J Hazard Mater 262, 634–641. https://doi.org/10.1016/j.jhazmat.2013.09.015.
[20] Liu, A., Zhao, Z., Qu, G., et al., 2018. Transformation/degradation of tetrabromobisphenol A and its derivatives: a review of the metabolism and metabolites. Environ Pollut Barking Essex 1987 243, 1141–1153. https://doi.org/10.1016/j.envpol.2018.09.068.
[21] Liu, G., Liu, S., Yang, J., et al., 2024. Complete biodegradation of tetrabromobisphenol A through sequential anaerobic reductive dehalogenation and aerobic oxidation. J Hazard Mater 470, 134217. https://doi.org/10.1016/j.jhazmat.2024.134217.
[22] Zhang, K.-H., Bao, L.-J., Wang, Y., et al., 2024. Effects of polymer matrix and temperature on pyrolysis of tetrabromobisphenol A: product profiles and transformation pathways. J Hazard Mater 474, 134806. https://doi.org/10.1016/j.jhazmat.2024.134806.
[23] Plattard, N., Dupuis, A., Migeot, V., et al., 2021. An overview of the literature on emerging pollutants: chlorinated derivatives of Bisphenol A (ClxBPA). Environ Int 153, 106547. https://doi.org/10.1016/j.envint.2021.106547.
[24] Albouy, M., Deceuninck, Y., Migeot, V., et al., 2023. Characterization of pregnant women exposure to halogenated parabens and bisphenols through water consumption. J Hazard Mater 448, 130945. https://doi.org/10.1016/j.jhazmat.2023.130945.
[25] Zhou, Y., Chen, M., Zhao, F., et al., 2015. Ubiquitous occurrence of chlorinated byproducts of bisphenol A and nonylphenol in bleached food contacting papers and their implications for human exposure. Environ Sci Technol 49, 7218–7226. https://doi.org/10.1021/acs.est.5b00831.
[26] Abou-Elwafa Abdallah, M., 2016. Environmental occurrence, analysis and human exposure to the flame retardant tetrabromobisphenol-A (TBBP-A)-a review. Environ Int 94, 235–250. https://doi.org/10.1016/j.envint.2016.05.026.
[27] Kalyvas, H., Andra, S.S., Charisiadis, P., et al., 2014. Influence of household cleaning practices on the magnitude and variability of urinary monochlorinated bisphenol A. Sci Total Environ 490, 254–261. https://doi.org/10.1016/j.scitotenv.2014.04.072.
[28] Munier, M., Grouleff, J., Gourdin, L., et al., 2016. In vitro effects of the endocrine disruptor p,p'DDT on human follitropin receptor. Environ Health Perspect. https://doi.org/10.1289/ehp.1510006.
[29] Foulkes, N.S., Schlotter, F., Pévet, P., Sassone-Corsi, P., 1993. Pituitary hormone FSH directs the CREM functional switch during spermatogenesis. Nature 362, 264–267. https://doi.org/10.1038/362264a0.
[30] Robker, R.L., Richards, J.S., 1998. Hormonal control of the cell cycle in ovarian cells: proliferation versus differentiation. Biol Reprod 59, 476–482. https://doi.org/10.1095/biolreprod59.3.476.
[31] Minegishi, T., Nakamura, K., Takakura, Y., et al., 1991. Cloning and sequencing of human FSH receptor cDNA. Biochem Biophys Res Commun 175, 1125–1130.
[32] Wrobel, J., Jetter, J., Kao, W., et al., 2006. 5-Alkylated thiazolidinones as follicle-stimulating hormone (FSH) receptor agonists. Bioorg Med Chem 14, 5729–5741. https://doi.org/10.1016/j.bmc.2006.04.012.

[33] Binkowski, B.F., Fan, F., Wood, K.V., 2011. Luminescent biosensors for real-time monitoring of intracellular cAMP. Methods Mol Biol Clifton NJ 756, 263–271. https://doi.org/10.1007/978-1-61779-160-4_14.
[34] Webb, B., Sali, A., 2016. Comparative protein structure modeling using MODELLER. Curr Protoc Protein Sci 86, 2.9.1–2.9.37. https://doi.org/10.1002/cpps.20.
[35] Duan, J., Xu, P., Cheng, X., et al., 2021. Structures of full-length glycoprotein hormone receptor signalling complexes. Nature 598, 688–692. https://doi.org/10.1038/s41586-021-03924-2.
[36] Sherman, W., Beard, H.S., Farid, R., 2006. Use of an induced fit receptor structure in virtual screening. Chem Biol Drug Des 67, 83–84. https://doi.org/10.1111/j.1747-0285.2005.00327.x.
[37] Sherman, W., Day, T., Jacobson, M.P., et al., 2006. Novel procedure for modeling ligand/receptor induced fit effects. J Med Chem 49, 534–553. https://doi.org/10.1021/jm050540c.
[38] Abraham, M.J., Murtola, T., Schulz, R., et al., 2015. GROMACS: High performance molecular simulations through multi-level parallelism from laptops to supercomputers. Softw 1–2 19–25. https://doi.org/10.1016/j.softx.2015.06.001.
[39] Huang, J., Rauscher, S., Nawrocki, G., et al., 2017. CHARMM36m: an improved force field for folded and intrinsically disordered proteins. Nat Methods 14, 71–73. https://doi.org/10.1038/nmeth.4067.
[40] Daura, X., Gademann, K., Jaun, B., et al., 1999. Peptide folding: when simulation meets experiment. Angew. Chem Int Ed 38, 236–240. https://doi.org/10.1002/(SICI)1521-3773(19990115)38:1/2<236::AID-ANIE236>3.0.CO;2-M.
[41] Fan, Z., Hu, J., An, W., Yang, M., 2013. Detection and occurrence of chlorinated byproducts of bisphenol a, nonylphenol, and estrogens in drinking water of china: comparison to the parent compounds. Environ Sci Technol 47, 10841–10850. https://doi.org/10.1021/es401504a.
[42] Cambien, G., Venisse, N., Migeot, V., et al., 2020. Simultaneous determination of bisphenol A and its chlorinated derivatives in human plasma: Development, validation and application of a UHPLC-MS/MS method. Chemosphere 242, 125236. https://doi.org/10.1016/j.chemosphere.2019.125236.
[43] Li, A., Zhuang, T., Shi, W., et al., 2020. Serum concentration of bisphenol analogues in pregnant women in China. Sci Total Environ 707, 136100. https://doi.org/10.1016/j.scitotenv.2019.136100.
[44] Cariou, R., Antignac, J.-P., Zalko, D., et al., 2008. Exposure assessment of French women and their newborns to tetrabromobisphenol-A: occurrence measurements in maternal adipose tissue, serum, breast milk and cord serum. Chemosphere 73, 1036–1041. https://doi.org/10.1016/j.chemosphere.2008.07.084.
[45] Dirtu, A.C., Roosens, L., Geens, T., et al., 2008. Simultaneous determination of bisphenol A, triclosan, and tetrabromobisphenol A in human serum using solid-phase extraction and gas chromatography-electron capture negative-ionization mass spectrometry. Anal Bioanal Chem 391, 1175–1181. https://doi.org/10.1007/s00216-007-1807-9.
[46] Dufour, P., Pirard, C., Charlier, C., 2017. Determination of phenolic organohalogens in human serum from a Belgian population and assessment of parameters affecting the human contamination. Sci Total Environ 599–600, 1856–1866. https://doi.org/10.1016/j.scitotenv.2017.05.157.
[47] Ho, K.-L., Yuen, K.-K., Yau, M.-S., et al., 2017. Glucuronide and sulfate conjugates of tetrabromobisphenol A (TBBPA): chemical synthesis and correlation between their urinary levels and plasma TBBPA content in voluntary human donors. Environ Int 98, 46–53. https://doi.org/10.1016/j.envint.2016.09.018.
[48] Grignon, C., Venisse, N., Rouillon, S., et al., 2016. Ultrasensitive determination of bisphenol A and its chlorinated derivatives in urine using a high-throughput UPLC-MS/MS method. Anal Bioanal Chem 408, 2255–2263. https://doi.org/10.1007/s00216-015-9288-8.
[49] Liao, C., Kannan, K., 2012. Determination of free and conjugated forms of bisphenol A in human urine and serum by liquid chromatography-tandem mass spectrometry. Environ Sci Technol 46, 5003–5009. https://doi.org/10.1021/es300115a.
[50] Wei, X., Hu, Y., Zhu, Q., et al., 2022. Co-exposure and health risks of several typical endocrine disrupting chemicals in general population in eastern China. Environ Res 204, 112366. https://doi.org/10.1016/j.envres.2021.112366.
[51] Xu, L., Hu, Y., Zhu, Q., et al., 2022. Several typical endocrine-disrupting chemicals in human urine from general population in China: regional and demographic-related differences in exposure risk. J Hazard Mater 424, 127489. https://doi.org/10.1016/j.jhazmat.2021.127489.
[52] Yanofsky, S.D., Shen, E.S., Holden, F., et al., 2006. Allosteric activation of the Follicle-stimulating Hormone (FSH) receptor by selective, nonpeptide agonists. J Biol Chem 281, 13226–13233. https://doi.org/10.1074/jbc.M600601200.
[53] Suteau, V., Briet, C., Lebeault, M., et al., 2020. Human amniotic fluid-based exposure levels of phthalates and bisphenol A mixture reduce INSL3/RXFP2 signaling. Environ Int 138, 105585. https://doi.org/10.1016/j.envint.2020.105585.
[54] Delfosse, V., Grimaldi, M., le Maire, A., et al., 2014. Nuclear receptor profiling of bisphenol-A and its halogenated analogues. Vitam Horm 94, 229–251. https://doi.org/10.1016/B978-0-12-800095-3.00009-2.
[55] Li, C.-H., Zhang, D.-H., Jiang, L.-D., et al., 2021. Binding and activity of bisphenol analogues to human peroxisome proliferator-activated receptor β/δ. Ecotoxicol Environ Saf 226, 112849. https://doi.org/10.1016/j.ecoenv.2021.112849.
[56] Suyama, K., Kaneko, S., Kesamaru, H., et al., 2020. Evaluation of the influence of halogenation on the binding of Bisphenol A to the estrogen-related receptor γ. Chem Res Toxicol 33, 889–902. https://doi.org/10.1021/acs.chemrestox.9b00379.
[57] Riu, A., Grimaldi, M., le Maire, A., et al., 2011. Peroxisome proliferator-activated receptor γ is a target for halogenated analogs of bisphenol A. Environ Health Perspect 119, 1227–1232. https://doi.org/10.1289/ehp.1003328.
[58] Zhuang, S., Zhang, C., Liu, W., 2014. Atomic insights into distinct hormonal activities of bisphenol A analogues toward PPARγ and ERα receptors. Chem Res Toxicol 27, 1769–1779. https://doi.org/10.1021/tx500232b.
[59] Kollitz, E.M., De Carbonnel, L., Stapleton, H.M., Lee Ferguson, P., 2018. The affinity of brominated phenolic compounds for human and zebrafish thyroid receptor β: influence of chemical structure. Toxicol Sci J Soc Toxicol 163, 226–239. https://doi.org/10.1093/toxsci/kfy028.
[60] Zheng, J., Chen, S., Lu, H., et al., 2024. Enhanced inhibition of human and rat aromatase activity by benzene ring substitutions in bisphenol A: QSAR structure-activity relationship and in silico docking analysis. J Hazard Mater 465, 133252. https://doi.org/10.1016/j.jhazmat.2023.133252.
[61] Lei, B., Tang, Q., Sun, S., et al., 2021. Insight into the mechanism of tetrachlorobisphenol A (TCBPA)-induced proliferation of breast cancer cells by GPER-mediated signaling pathways. Environ Pollut Barking Essex 1987 275, 116636. https://doi.org/10.1016/j.envpol.2021.116636.
[62] Lei, B., Xu, L., Huang, Y., et al., 2022. Chlorobisphenol A activated kisspeptin/GPR54-GnRH neuroendocrine signals through ERα and GPER pathway in neuronal GT1-7 cells. Ecotoxicol Environ Saf 233, 113290. https://doi.org/10.1016/j.ecoenv.2022.113290.
[63] Liu, X., Xue, Q., Zhang, H., et al., 2021. Structural basis for molecular recognition of G protein-coupled estrogen receptor by selected bisphenols. Sci Total Environ 793, 148558. https://doi.org/10.1016/j.scitotenv.2021.148558.
[64] Wang, L., Huang, C., Li, L., et al., 2023. In vitro and in silico assessment of GPER-dependent neurocytotoxicity of emerging bisphenols. Sci Total Environ 862, 160762. https://doi.org/10.1016/j.scitotenv.2022.160762.
[65] Aathi, M.S., Kumar, C., Prabhudesai, K.S., et al., 2022. Mapping of FSHR agonists and antagonists binding sites to identify potential peptidomimetic modulators. Biochim Biophys Acta Biomembr 1864, 183842. https://doi.org/10.1016/j.bbamem.2021.183842.
[66] De Pascali, F., Ayoub, M.A., Benevelli, R., et al., 2021. Pharmacological characterization of low molecular weight biased agonists at the follicle stimulating hormone receptor. Int J Mol Sci 22, 9850. https://doi.org/10.3390/ijms22189850.
[67] Arey, B.J., 2008. Allosteric modulators of glycoprotein hormone receptors: discovery and therapeutic potential. Endocrine 34, 1–10. https://doi.org/10.1007/s12020-008-9098-2.
[68] Stenkamp, R.E., 2008. Alternative models for two crystal structures of bovine rhodopsin. Acta Crystallogr D Biol Crystallogr D64 902–904. https://doi.org/10.1107/S0907444908017162.
[69] Duan, J., Xu, P., Zhang, H., et al., 2023. Mechanism of hormone and allosteric agonist mediated activation of follicle stimulating hormone receptor. Nat Commun 14, 519. https://doi.org/10.1038/s41467-023-36170-3.
[70] Schulze, A., Kleinau, G., Neumann, S., et al., 2020. The intramolecular agonist is obligate for activation of glycoprotein hormone receptors. FASEB J 34, 11243–11256. https://doi.org/10.1096/fj.202000100R.
[71] Ji, I., Ji, T.H., 1995. Differential roles of exoloop 1 of the human follicle-stimulating hormone receptor in hormone binding and receptor activation. J Biol Chem 270, 15970–15973. https://doi.org/10.1074/jbc.270.27.15970.
[72] Sohn, J., Ryu, K., Sievert, G., et al., 2002. Follicle-stimulating hormone interacts with exoloop 3 of the receptor. J Biol Chem 277, 50165–50175. https://doi.org/10.1074/jbc.M207646200.
[73] Lin, Y.-J., Lin, Z., 2020. In vitro-in silico-based probabilistic risk assessment of combined exposure to bisphenol A and its analogues by integrating ToxCast high-throughput in vitro assays with in vitro to in vivo extrapolation (IVIVE) via physiologically based pharmacokinetic (PBPK) modeling. J Hazard Mater 399, 122856. https://doi.org/10.1016/j.jhazmat.2020.122856.
[74] Caballero-Casero, N., Lunar, L., Rubio, S., 2016. Analytical methods for the determination of mixtures of bisphenols and derivatives in human and environmental exposure sources and biological fluids. A review. Anal Chim Acta 908, 22–53. https://doi.org/10.1016/j.aca.2015.12.034.
[75] Zhang, D., Liu, X., Qi, Y., et al., 2023. Binding, activity and risk assessment of bisphenols toward farnesoid X receptor pathway: In vitro and in silico study. Sci Total Environ 869, 161701. https://doi.org/10.1016/j.scitotenv.2023.161701.
[76] Andersen, M.E., 1995. Development of physiologically based pharmacokinetic and physiologically based pharmacodynamic models for applications in toxicology and risk assessment. Toxicol Lett 79, 35–44. https://doi.org/10.1016/0378-4274(95)03355-o.
[77] Ougier, E., Zeman, F., Antignac, J.-P., et al., 2021. Human biomonitoring initiative (HBM4EU): Human biomonitoring guidance values (HBM-GVs) derived for bisphenol A. Environ Int 154, 106563. https://doi.org/10.1016/j.envint.2021.106563.
[78] Riu, A., le Maire, A., Grimaldi, M., et al., 2011. Characterization of novel ligands of ERα, Erβ, and PPARγ: the case of halogenated bisphenol A and their conjugated metabolites. Toxicol Sci J Soc Toxicol 122, 372–382. https://doi.org/10.1093/toxsci/kfr132.
[79] Akiyama, E., Kakutani, H., Nakao, T., et al., 2015. Facilitation of adipocyte differentiation of 3T3-L1 cells by debrominated tetrabromobisphenol A compounds detected in Japanese breast milk. Environ Res 140, 157–164. https://doi.org/10.1016/j.envres.2015.03.035.
[80] Nakao, T., Akiyama, E., Kakutani, H., et al., 2015. Levels of tetrabromobisphenol A, tribromobisphenol A, dibromobisphenol A, monobromobisphenol A, and bisphenol a in Japanese breast milk. Chem Res Toxicol 28, 722–728. https://doi.org/10.1021/tx500495j.

[81] Wang, H., Sang, J., Ji, Z., et al., 2024. Halogenated bisphenol A derivatives potently inhibit human and rat 11β-hydroxysteroid dehydrogenase 1: structure-activity relationship and molecular docking. Environ Toxicol 39, 2560–2571. https://doi.org/10.1002/tox.24124.
[82] Yu, Y., Wang, M., Chen, Y., et al., 2023. Halogenated bisphenol A derivatives potently inhibit human, rat, and mouse gonadal 3β-hydroxysteroid dehydrogenases: Structure-activity relationship and in silico molecular docking analysis. Toxicol Lett 386, 20–29. https://doi.org/10.1016/j.toxlet.2023.09.002.
[83] Suyama, K., Kesamaru, H., Okubo, T., et al., 2023. High cytotoxicity of a degraded TBBPA, dibromobisphenol A, through apoptotic and necrosis pathways. Heliyon 9, e13003. https://doi.org/10.1016/j.heliyon.2023.e13003.
[84] Bhartiya, D., Patel, H., 2021. An overview of FSH-FSHR biology and explaining the existing conundrums. J Ovarian Res 14, 144. https://doi.org/10.1186/s13048-021-00880-3.
[85] Souter, I., Smith, K.W., Dimitriadis, I., et al., 2013. The association of bisphenol-A urinary concentrations with antral follicle counts and other measures of ovarian reserve in women undergoing infertility treatments. Reprod Toxicol Elmsford N 42, 224–231. https://doi.org/10.1016/j.reprotox.2013.09.008.
[86] Li, Y., Zhang, W., Liu, J., et al., 2014. Prepubertal bisphenol A exposure interferes with ovarian follicle development and its relevant gene expression. Reprod Toxicol Elmsford N 44, 33–40. https://doi.org/10.1016/j.reprotox.2013.09.002.
[87] Rodríguez, H.A., Santambrosio, N., Santamaría, C.G., et al., 2010. Neonatal exposure to bisphenol A reduces the pool of primordial follicles in the rat ovary. Reprod Toxicol Elmsford N 30, 550–557. https://doi.org/10.1016/j.reprotox.2010.07.008.
[88] Zhang, H.-Q., Zhang, X.-F., Zhang, L.-J., et al., 2012. Fetal exposure to bisphenol A affects the primordial follicle formation by inhibiting the meiotic progression of oocytes. Mol Biol Rep 39, 5651–5657. https://doi.org/10.1007/s11033-011-1372-3.
[89] Bloom, M.S., Kim, D., Vom Saal, F.S., et al., 2011. Bisphenol A exposure reduces the estradiol response to gonadotropin stimulation during in vitro fertilization. Fertil Steril 96, 672–677.e2. https://doi.org/10.1016/j.fertnstert.2011.06.063.
[90] Paoli, D., Pallotti, F., Dima, A.P., et al., 2020. Phthalates and Bisphenol A: presence in blood serum and follicular fluid of Italian women undergoing assisted reproduction techniques. Toxics 8, 91. https://doi.org/10.3390/toxics8040091.
[91] Lei, B., Yang, Y., Xu, L., et al., 2024. Molecular insights into the effects of tetrachlorobisphenol A on puberty initiation in Wistar rats. Sci Total Environ 911, 168643. https://doi.org/10.1016/j.scitotenv.2023.168643.